ISSN 0915-6348

NATIONAL INSTITUTE FOR FUSION SCIENCE

Plasma Heating and Current Drive

T. Watari

(Received - Aug. 25, 1997)

NIFS-PROC-35 Oct. 1997

RESEARCH REPORT
NIFS-PROC Series

NAGOYA, JAPAN

Plasma Heating and Current Drive

T. Watari

National Institute for Fusion Science
Nagoya, 464-01, Japan

Abstract

Plasma heating is one of the very important aspects of nuclear fusion research, by which plasma is heated up to a few 10's of keV to obtain large enough fusion reaction rate to sustain chain reaction. Among the heating methods examined in the past in the experiments Electron Cyclotron Heating, Ion Cyclotron Heating, Lower Hybrid Heating, and Neutral Beam Heating were proven their usefulness. They have their own unique features and, therefore, survived their competition in tokamak experiments. This lecture intend to give the audience some essence of the physics related to Plasma Heating to help understand intriguing evolution of this field in the past and new applications. The lecture will also refer to the fact that the same heating methods can be used in driving current in plasmas. Current drive is important idea to facilitate steady state tokamak reactor. This lecture also gives a handy account of the mechanism of current drive, requirement of the current drive efficiency, and an assessment of achievable maximum current drive efficiencies in the future.

This article was prepared for the lecture at "Frontier of Physics in Fusion Relevant Plasmas", 1996 Asian Science Seminar, 20-29 October 1996, Hefei - Tunxi, Anhui Province, P.R. China.

Key words
Plasma Heating, ECH, ICH, ICRF, LHH, IBWH, NBI, ECCD, fast wave current drive, LHCD, NBCD, current drive efficiency, wave dispersion relation, wave absorption

Plasma Heating and Current Drive

T.Watari
National Institute for Fusion Science

Introduction

Plasma heating and current drive have been intensively investigated in the past several decades. They have been key issues in thermonuclear fusion research using various kind of confinement concepts including tokamaks, helical systems, and open end systems. These experimental and theoretical investigations identified following four methods of plasma heating and clarified their heating mechanisms to a considerable extent.
1)NB; Neutral Beam Injection Heating(CD)
2)ECH; Electron Cyclotron Heating(CD)
3)LHH; Lower Hybrid Heating(CD)
4)ICH; Ion cyclotron Heating(CD)
5)AW; Alfven Wave Heating(CD)
The physics of NBI is rather straightforward. It has been widely used and has been the most reliable heating scheme. The deposition profile of NBI is determined depending on the beam energy, plasma density, and the size of the device. As an example of efforts to optimize power deposition profile, we note that the injection energy of NBI is increasing according to the increasing size of the devices. To do this, development of negative ion based neutral beam injector is one technological challenge in recent NBI related researches; ordinary positive ion based NBI loses efficiency as acceleration energy increases.
The other methods all use plasma waves in order to deliver the power into the core of the plasma. Each of them has its own merits and demerits. Even today when launching ITER project is being discussed, selecting just one method and discarding others seems to be difficult. Combination of these methods should rather be considered because of envisaged interesting synergies .
The same heating schemes 1)~5) can be used as schemes of driving currents in the plasma. Current drive is particularly important for tokamaks and various non inductive current drive schemes have been demonstrated in the experiments. However, in the tide to re-examine the economic feasibility of fusion power plant as stimulated by the ITER activity, current drive efficiency and its improvement is gathering critical attention. Demonstration of the boot strap current encouraged such non inductive current drive. It reduces the circulating power of a fusion plant according to the reduced fraction of the current that is undertaken by non inductive current drive. In recent researches, current profile optimization for boot strap current is being considered making the bootstrap fraction larger.
Part I of this course is allotted to introduction of the basic ideas necessary for investigation of plasma heating and current drive. The physics involved in NBI is relatively simple and it is referred only to fulfil self containedness. Experimental results of plasma heating will not be covered in this short text, though magnificent progress has been made in this field.
The first half of Part -II will be allotted to explanation of mechanisms and efficiencies of various current drive schemes. In the later half of Part-II, Experimental achievement of these current drive schemes will be summarized. Boot strap current is an non-ignorable factor in recent nuclear fusion research. It's role among other noninductive current drive schemes is discussed at the end of Part-II together with the prospects of respective current drive schemes.
Before we move to the text, we put the "golden rule" for plasma heating.

1) Deliver the heat deep into the core of the plasma.
2) Keep interaction between waves and plasma at the edge low.
3) Keep one pass absorption of the wave reasonably high.
4) Improve the confinement of high energy particles.
5) Enhance energy relaxation between high energy particles and bulk ions.
6) Condition wall and choose proper material from where impurities come in.
In general, these conditions are satisfied easier as the size of the device increases. They will be satisfied in reactors or even in existing large sized devices and we can loosen some of these rules. The use of this flexibility in improvement of energy confinement, stability of the plasma, and other required performances for a reactor is very interesting aspect of plasma heating and current drive. Though, some interesting results from this field of research were introduced in this course, such materials are not incorporated in this text for it would need another article.

Part I. Basic knowledge for wave heating

This section gives a brief introduction to wave physics as base of understanding plasma heating. The following contents can be explained referring to the standard texts[1-2].

I.1 Dielectric tensor

Wave propagation in a plasma is given as solutions to the Maxwell's equation:

$$\mathrm{rot}\vec{B} = \frac{1}{c}\frac{\partial E}{\partial t} + 4\pi\vec{j} \qquad --(1)$$

$$\mathrm{rot}\vec{E} = -\frac{1}{c}\frac{\partial \vec{B}}{\partial t} \qquad --(2)$$

, where $\vec{E}$, $\vec{B}$, and $\vec{j}$ are electric field, magnetic field and current density, respectively.
The propagation of electric waves in vacuum has been studied by many authors. The only difference between waves in plasma and those in vacuum is that the Maxwell equation Eq.(1) has RF current $\vec{j}$ in the right hand side. For plasma has high electrical conductivity, presence of electric field associated with the wave causes the rf currents. In most of the cases, the confinement system itself has equilibrium magnetic field and current and the wave is taken as perturbations on such equilibrium quantities. Therefore, waves can be taken as small quantity making the equations linear integro-differential equations,

$$\vec{j}(r,t) = \int_{-\infty}^{t}\int \vec{\sigma}(r,r',t,t')\cdot\vec{E}(r',t')\,dt'\,d^3r' \qquad --(3)$$

where, $\vec{\sigma}$ is called conductivity tensor. If the plasma is uniform and steady, the dielectric conductivity tensor may be written as functions of r-r' and t-t' only:

$$\vec{j}(r,t) = \int_{-\infty}^{t} \int \sigma(r-r', t-t')\, E(r', t')\, dt'\, d^3r' \quad --(4)$$

And, when Fourier transformed, it is written as

$$\vec{j}(k,\omega) = \bar{\sigma}(k,\omega) \cdot \vec{E}(k,\omega) . \quad --(5)$$

According to the form of the right hand side of Eq.(1), it is convenient to define vector $\vec{D}$ by

$$\frac{1}{c}\frac{\partial \vec{D}}{\partial t} = \frac{1}{c}\frac{\partial \vec{E}}{\partial t} + 4\pi\vec{j} . \quad --(6)$$

Dielectric tensor $\bar{\varepsilon}$ is then defined by

$$\vec{D} = \bar{\varepsilon}(\vec{k},\omega) \cdot \vec{E} . \quad --(7)$$

Obviously, the conductivity tensor and dielectric tensor are related by

$$\bar{\varepsilon} = \bar{I} - \frac{4\pi}{i\omega}\bar{\sigma}(\vec{k},\omega) . \quad --(8)$$

Thus , the characteristics of a plasma as wave propagating media is described solely either by $\bar{\sigma}$ or $\bar{\varepsilon}$.

I.2 Dispersion relation of waves

If we separate the current of Eq.(1) into sum of externally applied specified current and the current induced by the electric field, the total current $\vec{j} = \vec{j}_{total}$ may be written as

$$\vec{j} = \vec{j}_{spec} + \vec{j}_{ind} . \quad --(9)$$

Eliminating $\vec{B}$ by substituting Eq.(2) into Eq.(1), one gets

$$\vec{D} \bullet \vec{E} = 4\pi\frac{c}{i\omega}\vec{j}_{ext} \quad --(10)$$

with

$$\vec{D} = \vec{n}\vec{n} - n^2 I + \bar{\varepsilon} \quad --(11)$$

and

$$\vec{n} = \frac{c\vec{k}}{\omega} \quad . \quad --(12)$$

Multiplying Eq.(10) by $\vec{D}^{-1}$ from the left hand side, one gets

$$\vec{E} = 4\pi \frac{c}{i\omega} \vec{D}^{-1} \cdot \vec{j}_{ext}\left(k, \omega\right) \quad . \quad --(13)$$

In general, this equation predicts large classes of forced oscillation problems.
Without external current, Eq.(10) reduces to

$$\vec{D} \bullet \vec{E} = 0 \quad -- \ (14)$$

or, in terms of dielectric elements,

$$\begin{pmatrix} \varepsilon_{xx} - n_z^2 - n_y^2 & \varepsilon_{xy} + n_x n_y & \varepsilon_{xz} + n_x n_z \\ \varepsilon_{yx} + n_y n_x & \varepsilon_{yy} - n_z^2 - n_x^2 & \varepsilon_{yz} + n_y n_z \\ \varepsilon_{zx} + n_z n_x & \varepsilon_{zy} + n_z n_y & \varepsilon_{zz} - n_x^2 - n_y^2 \end{pmatrix} \begin{pmatrix} E_x \\ E_y \\ E_z \end{pmatrix} = 0 \quad . \quad --(15)$$

Non trivial waves solution should satisfy

$$\left|\vec{D}\right| = 0 \, . \quad --(16)$$

This equation gives an interrelationship between the wave frequency ω and wave number $\vec{k}$ and, for this reason, it is called dispersion relation.

I.3 Cold approximation

If the wave length is sufficiently long, the current at a given point is simply proportional to the electric field at that point. An extreme limit of such case is called cold approximation and simply given by use of following Newtonian equation of motion.

$$m\frac{d\vec{v}}{dt} = q\left(\vec{E} + \frac{1}{c}\left[\vec{v} \times \vec{B}\right]\right) \, . \quad --(17)$$

Plasma current is obtained by

$$\vec{j} = \sum_s n_s q_s \vec{v}_s \quad --(18)$$

by using the solution to the Eq.(17). It is not difficult to derive the dielectric tensor

$$\vec{\varepsilon} = \begin{pmatrix} S & -iD & 0 \\ iD & S & 0 \\ 0 & 0 & P \end{pmatrix} \quad --(19)$$

with

$$S = \frac{1}{2}(R + L) \quad --(20)$$

$$D = \frac{1}{2}(R - L) \quad --(21)$$

$$R = 1 - \sum_s \frac{\omega_{ps}^2}{\omega(\omega + \Omega_s)} \quad --(22)$$

$$L = 1 - \sum_s \frac{\omega_{ps}^2}{\omega(\omega - \Omega_s)} \quad --(23)$$

and

$$P = 1 - \sum_s \frac{\omega_{ps}^2}{\omega^2} . \quad --(24)$$

I.4 Dielectric tensor of warm plasma

If wave length is not long enough the cold approximation is not valid. The following Vlasov equation is used in deriving an adequate dielectric tensor.

$$\frac{\partial f}{\partial t} + \vec{v} \cdot \nabla f + \frac{q}{m}\left(\vec{E} + \frac{1}{e}[\vec{v} \times \vec{B}]\right) \cdot \frac{\partial f}{\partial \vec{v}} = 0 \quad --(25)$$

It is suggested that readers may find expressions for dielectric tensor elements from other textbooks[1, 2].

$$\tilde{\varepsilon} = \begin{pmatrix} \varepsilon_{xx} & \varepsilon_{xx} & \varepsilon_{xx} \\ \varepsilon_{yx} & \varepsilon_{yy} & \varepsilon_{yz} \\ \varepsilon_{zx} & \varepsilon_{zy} & \varepsilon_{zz} \end{pmatrix} \quad --(26)$$

It is noted that $\varepsilon_{xz} = \varepsilon_{-zx}$ and $\varepsilon_{yz} = \varepsilon_{-zy}$ are not zero different from the cold approximation. Important features appearing in warm plasma approximations are Doppler shift and finite Larmour radius effects.

The dielectric tensor are separated in an Hermitian part $\tilde{\varepsilon}^{H}$ and an anti Hermetian part $\tilde{\varepsilon}^{A}$:

$$\tilde{\varepsilon} = \frac{\varepsilon + \varepsilon^{+}}{2} + i\frac{\varepsilon - \varepsilon^{+}}{2i} = \varepsilon_{H} + i\varepsilon_{A} \quad --(27)$$

The former is related to the reactive response of the plasma and the latter is related to the dissipative response. In order for waves to be well defined, an inequality

$$\varepsilon_{Hij} \gg \varepsilon_{Aij} \quad --(28)$$

has to be satisfied.

I.5 Waves often used in plasma heating and current drive

The waves are expressed by dispersion relation introduced by Eq.(16). In plasma heating various kind of waves are used as means to deliver the energy to the core of the plasma. This section briefly reviews these useful waves. It is convenient to classify the waves by their frequency ranges:

1) Electron Cyclotron Frequency Range: $\omega \sim \omega_{c,e}$

2) Lower Hybrid Frequency Range: $\omega_{c,i} < \omega < \omega_{c,e}$

3) Ion Cyclotron Range of Frequency: $\omega \sim \omega_{c,i}$

4)Alfven Wave Frequency Range: $\omega < \omega_{c,i}$

In the early phase of the radio-frequency heating such as model-C stellarator, the researchers were mostly interested in wave propagation along the magnetic field. However, in the recent experiments in tokamaks they are more interested in the wave propagation nearly perpendicular to the magnetic field. Therefore, in this short article, we usually limit our scope to the perpendicular propagation of the waves.

Figures.1 through 5 are the dispersion relations calculated for corresponding frequency regime. A magnetic configuration similar to a tokamak is assumed in the calculation, i.e., BT varies as 1/R with, R, the major radius. A parabolic density profile is assumed; the density is high at the center of the plasma and low at the periphery.

a) Waves Used in Electron Cyclotron Heating

The waves are classified into two categories: ordinary wave and extraordinary wave. The wave which has wave electric field parallel to the magnetic field is called Ordinary mode and the one with electric field perpendicular to the magnetic field is called Extraordinary mode.

a-1) Ordinary Wave

Fig.1 shows the dispersion relation of the Ordinary mode in ECH Frequency range.
This wave is often used in Electron Cyclotron Heating and is popular because it is used in plasma density measurement. The dispersion relation is given by

$$n_{\perp}^2 = 1 - \frac{\omega_{p,e}^2}{\omega^2}. \quad --(30)$$

We know from Eq.(30) that there is cut off density above which wave cannot penetrate. If the electron cyclotron is placed at the center of the plasma for the plasma heating purpose, the density limit is given by

$$\omega_{p,e}^2 = \omega^2 = \omega_{c,e}^2. \quad --(31)$$

It is necessary to increase the frequency together with the applied magnetic field.

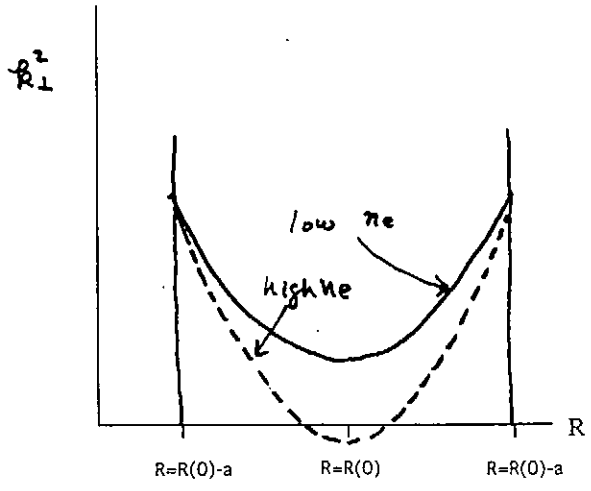

Fig.1 $N_\perp^2$ calculated for ordinary mode across the plasma on the equatorial plane

a-2 Extra-Ordinary Wave

Figure 2 shows the dispersion relation of the Extra-ordinary mode in EC frequency range: This wave also is often used in electron cyclotron heating.
The dispersion relation of the extra -ordinary mode is given by

$$n_\perp^2 = 1 - \frac{\omega_{p,e}^2}{\omega^2}\left\{1 + \frac{\omega_{c,e}^2}{\omega^2 - \omega_{p,e}^2 - \omega_{c,e}^2}\right\}. \quad --(32)$$

Cut off density is given by

$$\omega^2 = \omega_{p,e}^2 + \frac{\omega_{c,e}^2 + \sqrt{\omega_{c,e}^2 + 4\omega_{c,e}^2\omega_{p,e}^2}}{2}. \quad --(33)$$

As is very clear from Fig.2, the wave incident from the low field side meets cut off layer. Therefore, injection of the wave from high field side is often employed so that the waves reach the electron-cyclotron layer. Considerable power is absorbed there and the undamped wave may further meets the resonance layer,

$$\omega^2 = \omega_{p,e}^2 + \omega_{c,e}^2. \quad --(34)$$

The wave amplitude increases with its increased $k_\perp$ at the resonance layer and wave absorption

is intensified . The density limit of the fundamental extra-ordinary mode is twice as large as the density limit of the ordinary mode.

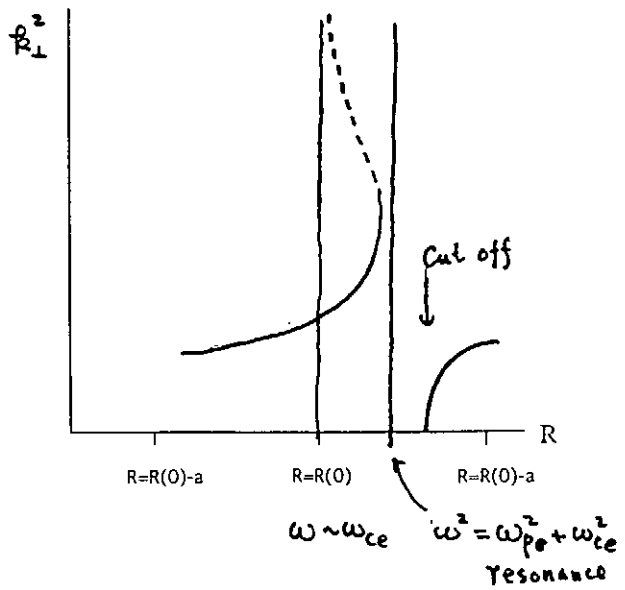

Fig.2 $N_\perp^2$ calculated for Extra-ordinary mode across the plasma on the equatorial plane

b) Waves used in Lower Hybrid Heating

Fig. 3 and 4 shows the dispersion relation of the waves in Lower Hybrid Frequency Range. In this frequency range, people take a convention of classifying the waves into slow wave and fast wave. When electro-static approximation is valid the simplest form of the Lower Hybrid wave is expressed by

$$\frac{k_\perp^2}{k_\parallel^2} = \left\{ \frac{m_i/m_e}{((\omega/\omega_{LH})^2 - 1)} \right\} \quad --(35)$$

with

$$\omega_{LH}^2 = \frac{\omega_{p,i}^2}{1 + \omega_{p,e}^2/\omega_{c,e}^2}. \quad --(36)$$

However, in a little more detailed analysis it is shown that waves in this frequency range are critically modified depending on their $k_{//}$ value.
Fig.3 shows the wave dispersion relation calculated for large $k_{//}$:

$$N_\parallel > (1 - \omega^2/\omega_{c,e}\omega_{c,i})^{-1}. \quad --(37)$$

Similarly, Fig.4 shows the wave dispersion relation calculated for small $k_{//}$.

$$N_{\parallel} < (1 - \omega^2/\omega_{c,e}\,\omega_{c,i})^{-1}. \quad --(38)$$

It is interesting to note that the lower hybrid heating was originally proposed for ion heating: For large $k_{//}$, the wave incident from the low field side meets so called lower hybrid layer where ions are expected to be heated. However, if the wave damping due to electron is high enough, wave is damped before it reaches the resonance layer and results in electron heating. The first observation in experiment was interaction of the wave with electrons. More exactly, there was the unexpected demonstration of current drive completely different from demonstration of electron heating. Since then, the wave of this frequency range was successfully used for current drive. However, it is known that there is density limit of the current drive, which may be associated with the accessibility of the LH wave to the plasma core.

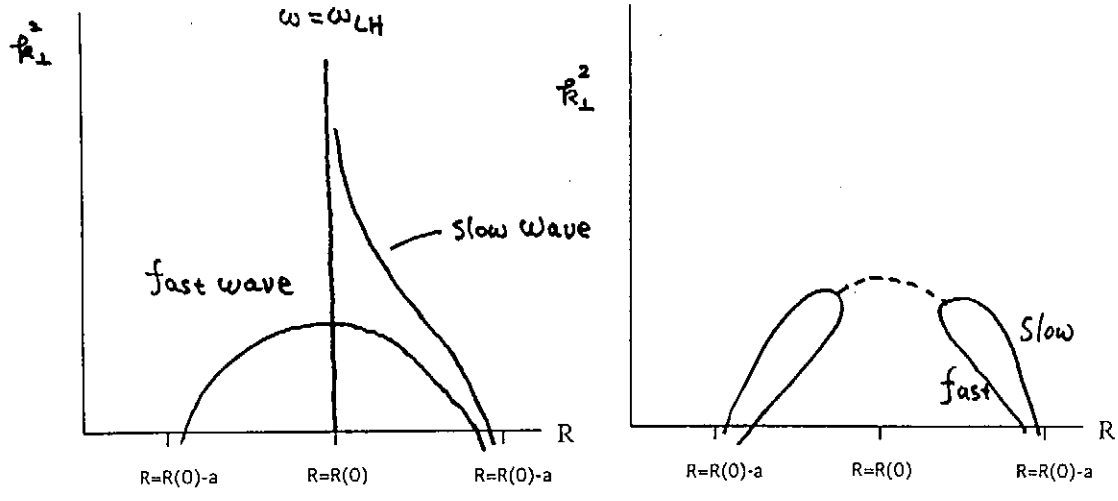

Fig.3 $N_\perp^2$ of slow and fast wave in Lower Hybrid Frequency Range: Large N// case

Fig.4 $N_\perp^2$ of slow and fast wave in Lower Hybrid Frequency Range: small N// case

c) Waves used in Ion cyclotron range of Frequency

c-1 fast wave

In the ion cycrotron frequency range, waves are classified into electromagnetic wave and electrostatic wave. The former is compressional Alfven Wave, which is obtained with an approximation that plasma conductivity along the magnetic lines of force is large compared to other components. Necessarily, the electric field in that direction is very small. The simplest form of the dispersion relation of the fast wave is given by

$$k_{\perp}^2 + k_{\parallel}^2\left(1 + \frac{\omega}{\omega_{c,i}}\right) = \left(\omega^2 / v_A^2\right). \quad --(39)$$

Figure.4 shows the wave dispersion relation for the electro-magnetic waves. For the present, the interested is in the heating of fuel ions in the plasma so the ion cyclotron resonance is placed on the plasma axis. A resonance layer is found in the low density region satisfying $\omega < \omega_{c,i}$ associated with Shear Alfven Wave. This branch is the one used in the classical Ion Cyclotron Resonance Heating in model-C stellarator. It is not preferred in present day tokamaks for it does not have accessibility to the plasma core. The other branch extending to the major part of the high density is called compressional Alfven wave. It has a good accessibility to the core. However, it is known that the wave polarization at the cyclotron layer is right handed circularly polarized and therefore ion heating is not strong.

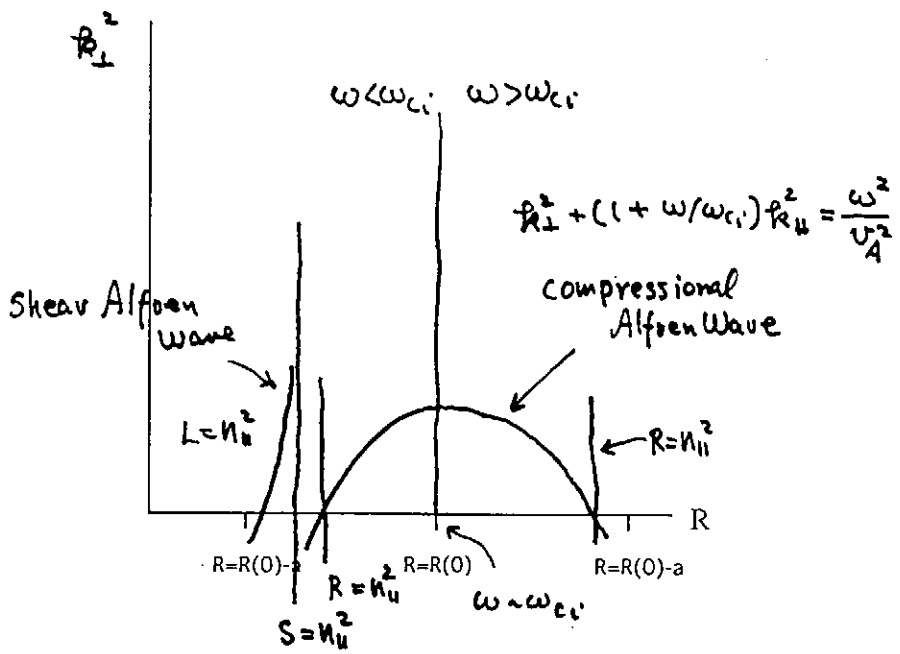

Fig.5 $N_{\perp}^2$ of fast wave in Ion Cyclotron Frequency Range

Figure.6 show the dispersion relation for the case that small amount of impurity ions are mixed into the majority fuel ions; the frequency is adjusted to the ion cyclotron frequency of minority ions at the plasma center. Then the wave has reasonably high component of left hand circularly polarization. Minority ions are heated in the interaction with RF and absorbed power is given to fuel ions via collision. If the concentration of the minority ions exceeds some critical value the plasma is divided into two propagation regions as can be easily studied in Fig.6. The wave incident from the high field side meets the resonance layer which is referred to as two ion hybrid layer. The dispersion relation has to be obtained in the full calculation of

$$n_{\perp}^2 = \frac{(R - n_{\parallel}^2)(L - n_{\parallel}^2)}{(S - n_{\parallel}^2)} \quad --(40)$$

including the minority ions. Readers are requested to see references[3] for more details. The wave is absorbed at the resonance layer via electron Landau damping and remaining wave energy is mode converted to Ion Bernstein Wave. Ray tracing analysis [4,5]which have been powerful method for EC and LH frequency range in calculating power deposition profile is not always valid in the ICRF. Full wave codes have been developed for analysis of ICRF waves[6,7].

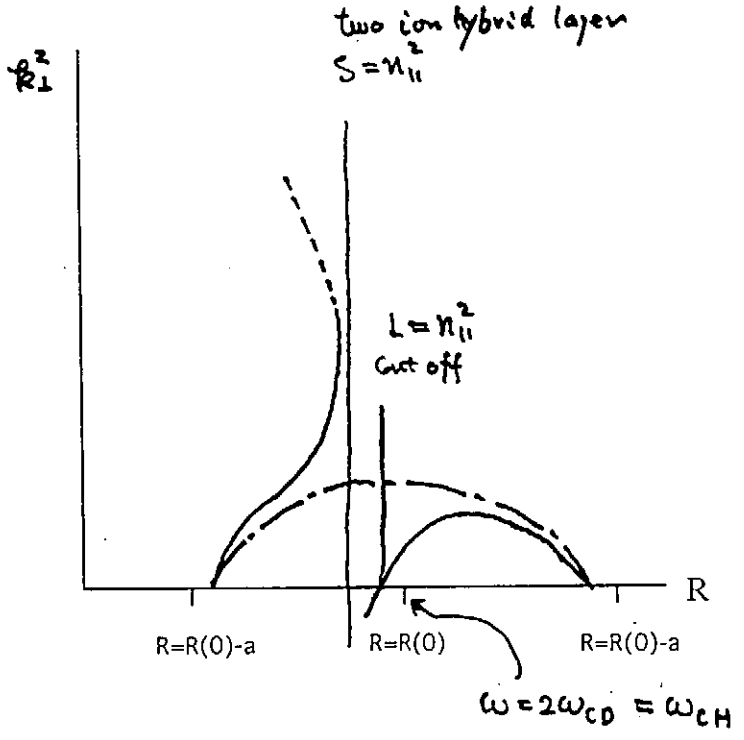

Fig6. $N_{\perp}^2$ of fast wave in Ion Cyclotron Range of Frequency when hydrogen minority ion is added to Deuterium plasma.

c-2 Slow wave (Ion-Bernstein Wave)

Figure.7 is the dispersion relation of the slow wave, i.e. Ion Bernstein Wave.
This wave is electro-static wave. There is a branch of Ion Bernstein wave for each adjacent pair of harmonics. We have to choose an adequate branch which has cyclotron harmonic layer at the center of the plasma and has small wave number at the edge of the plasma where wave is excited[8].

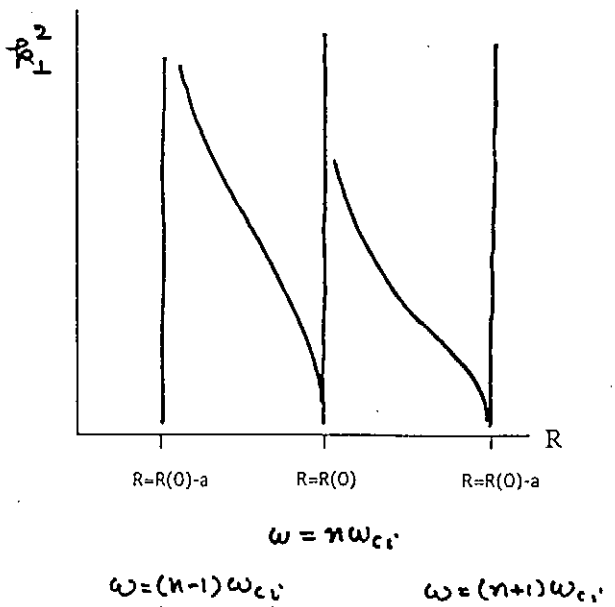

Fig.7. $N_\perp^2$ of Ion Bernstein Wave across the plasma cross section

d). Wave in Alfven Frequency Range:

Detailed explanation of the Alfven frequency range is expected to be given in the course given by Dr. Amagishi during this seminar.

Section -I.6 conservation equation

It is known that there is a kind of conservation law for wave propagating in weakly inhomogeneous plasma:

$$\frac{\partial W}{\partial t} + \nabla \cdot \vec{S} + Q = Q_{ext} . \quad --(41)$$

Here, involved quantities are defined as

$$W = \frac{1}{4\mu_0} \vec{B}^* \cdot \vec{B} + \frac{\varepsilon_0}{4} \vec{E}^* \cdot \frac{\partial \omega \vec{\varepsilon}^h}{\partial \omega} \cdot \vec{E} , \quad --(42)$$

$$\vec{S} = \frac{1}{4}\left(\vec{E} \times \vec{H}^* + \vec{E}^* \times \vec{H}\right) - \frac{\omega \varepsilon_0}{4} \frac{\partial \vec{\varepsilon}^h_{\alpha\beta}}{\partial \vec{k}} E^*_\alpha E_\beta, \quad --(43)$$

$$Q = \frac{\varepsilon_0}{2} \omega \vec{E}^* \cdot \vec{\varepsilon} \cdot \vec{E}, \quad --(44)$$

$$Q_{ex} = -\frac{1}{4}\left(\vec{j}^*_{ex} \cdot \vec{E}_{ex} + \vec{j}_{ex} \cdot \vec{E}^*_{ex}\right), \quad --(45)$$

and

$$\vec{\varepsilon}_{\alpha\beta} = \vec{\varepsilon}^h_{\alpha\beta} + i\vec{\varepsilon}^a_{\alpha\beta}. \quad --(46)$$

Equation(41) is regarded as wave energy conservation law.
Similarly , there is momentum conservation law which is expressed as:

$$\frac{\partial \vec{G}}{\partial t} + \nabla \cdot \vec{\vec{T}} + \vec{F} = \vec{F}_{ex}. \quad --(47)$$

Here,

$$\vec{G} = \frac{\varepsilon_0 \mu_0}{2} \mathrm{Re}\left[\left(\vec{\varepsilon}^h \cdot \vec{E}\right) \times \vec{H}^*\right] + \frac{\varepsilon_0}{4} \vec{k} \frac{\partial \vec{\varepsilon}^h}{\partial \omega} : \vec{E}^* \vec{E} \quad --(48)$$

$$\vec{\vec{T}} = -\frac{1}{2} \mathrm{Re}\left(\vec{E}^* \varepsilon_0 \vec{\vec{K}} \cdot \vec{E} + \mu_0 \vec{H}^* \vec{H}\right) + \frac{1}{4}\left(1 - \vec{k} \frac{\partial}{\partial \vec{k}}\right)\left(\varepsilon_0 \vec{\varepsilon}^h : \vec{E}^* \vec{E} + \mu_0 \vec{H}^* \cdot \vec{H}\right) \quad --(49)$$

$$\vec{F} = \frac{\vec{k} \varepsilon_0}{2} \vec{E} \cdot \vec{\varepsilon} \cdot \vec{E} --(50)$$

and

$$\vec{F}_{ex} = -\frac{1}{2} \mathrm{Re}[\rho_{ex} \vec{E}^* + \vec{j}_{ex} \times \mu_0 \vec{H}^*]. \quad --(51)$$

We find, from the comparison of Eq.(41) and Eq.(47), that there are correspondences:

$$\vec{S}, \text{ vs. } \vec{\vec{T}} = \vec{S} \frac{\vec{k}}{\omega} \quad ---(52)$$

$$W, \text{ vs. } \vec{G} = W \frac{\vec{k}}{\omega} \quad ---(53)$$

and

$$Q, \text{ vs. } \vec{F} = \frac{\vec{k}}{\omega} Q \ . \quad --(54)$$

They suggest that we may employ an analogy of quantum mechanics: a wave have momentum $\vec{p} = \hbar \vec{k}$ and energy $E = \hbar \omega$. Here, $\hbar$ may be any small value.

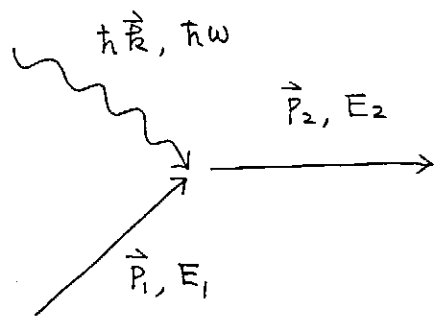

Fig.8 : Wave momentum conservation in wave particle interaction

I.7 Quasi-linear Fokker-Planck Equation

Wave particle interaction is more adequately treated with Quasi-linear Fokker-Planck Equation,

$$\frac{\partial f}{\partial t} = \left(\frac{\partial f}{\partial t}\right)_{coll} + \left(\frac{\partial f}{\partial t}\right)_{RF} + \left(\frac{\partial f}{\partial t}\right)_{trans} . \quad ---(55)$$

Terms on the right hand sides are, from the left, the change of distribution function due to collisions[10], due to interaction with the waves[9], and due to spatial transport. The last terms can be neglected in many cases. The second term has a form

$$\left(\frac{\partial f}{\partial t}\right)_{RF} = \frac{\partial}{\partial p} \cdot \tilde{D} \cdot \frac{\partial}{\partial p} f \quad --(56)$$

with

$$\bar{D} = \frac{1}{V} \sum_{n=-\infty}^{n=+\infty} \pi q^2 \int \frac{d^3k}{(2\pi)^3} \delta(\omega - k_\parallel v_\parallel - n\omega) \bar{a}^*_{k,n} \bar{a}_{k,n} \quad --(57)$$

where

$$\bar{a}_{k,n} = \frac{1}{\omega} (\varepsilon_{k,n} + \frac{p_\parallel}{p_\perp} J_n E_{z,n})(n\Omega \hat{e}_\perp + k_\parallel v_\perp \hat{e}_\parallel) \quad --(58)$$

with

$$\varepsilon_{k,n} = \frac{1}{\sqrt{2}} (\varepsilon^+_k J_{n+1} + \varepsilon^-_k J_{n-1}) \quad --(59)$$

and

$$\varepsilon^\pm = \frac{1}{\sqrt{2}} (E_{x,k} \pm iE_{y,k}) . \quad --(60)$$

The summation with respect to n represents various wave particle interactions: n=0 term contains both Landau damping and transit time damping. n=1 term corresponds to fundamental cyclotron damping, and terms with n>1 correspond to higher harmonic damping.
The presence of the delta-function in Eq.(57) means that the wave particle interaction occurs when resonance condition is satisfied.

$$\omega - n\omega_c = k_\parallel v_\parallel \quad -(61)$$

Using Eq.(58 and 61) , Eq.(56) is interpreted that the gradient of distribution function in the direction of

$$\vec{s} = n\omega_c \hat{e}_\perp + k_\parallel v_\perp \hat{e}_\parallel \quad --(62)$$

causes a flow in the direction of $\vec{s}$. And the divergence of the flow gives the net change of the distribution function. Thus the stream lines of particles in the velocity space is given by

$$\frac{\delta p_\parallel}{\delta p_\perp} = \frac{k_\parallel v_\parallel}{\omega - k_\parallel v_\parallel} \quad --(63)$$

which is integrated to give a family of concentric circles. In Fig.(9), shown are the interaction zone given by Eq.(61) and the a family of stream lines[11]:

$$v_\perp^2 + (v_\parallel - \omega / k_\parallel)^2 = \text{const} \quad --(64)$$

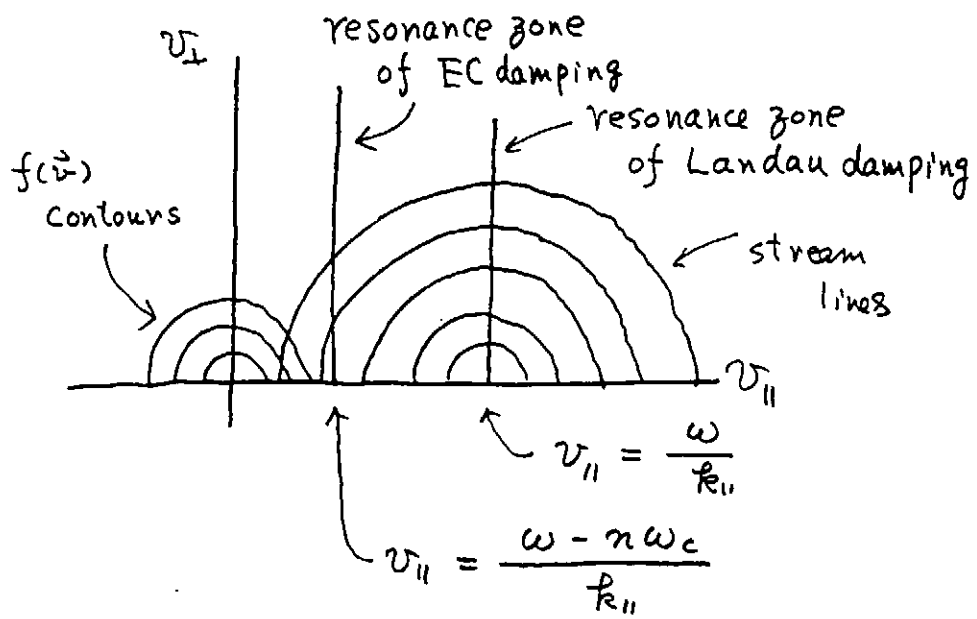

Fig.9 The stream lines showing the direction of the kick and the interaction zone.

I.8 Wave damping mechanisms:

a) Ion cyclotron damping and higher harmonic damping

For simplicity let us consider ion cyclotron damping; similar treatment is made for it's counter part, electron cyclotron damping.
According to the discussion in section (I.7) and from the inspection of Eq.(58), relevant quasi-linear kick term is simplified as

$$\frac{\partial f}{\partial t} = \frac{\partial}{\partial p_\perp} D_\perp \frac{\partial}{\partial p_\perp} f \quad ---(65)$$

where

$$D_\perp = \sum_{n=-\infty}^{n=+\infty} \pi q^2 \int \frac{d^3k}{(2\pi)^3} \delta(\omega - n\omega_c - k_\parallel v_\parallel) \frac{1}{2} |\varepsilon^-|^2 J_{n-1}^2 \quad --(66)$$

The Bessel function in Eq.(66) stands for finite Larmour radius effects. The Bessel function is expanded for n=1, n=2, and n=N as follows:

n=1 : Fundamental ion cyclotron heating

$$J_0\left(\frac{1}{2} k_\perp^2 \rho_i^2\right) \sim 1 \quad --(67)$$

n=2 : Second cyclotron harmonic heating

$$J_1(\frac{1}{2}k_\perp^2\rho_i^2) \sim \frac{1}{2}k_\perp^2\rho_i^2 \quad --(68)$$

n=N: N-th cyclotron harmonic heating

$$J_1(\frac{1}{2}k_\perp^2\rho_i^2) \sim \frac{1}{(N-1)!}(\frac{1}{2})^{N-1}(\frac{1}{2}k_\perp^2\rho_i^2) \quad --(69)$$

It is clear from this expression that cyclotron damping becomes weak with increasing harmonic number. This is the case particularly for fast waves where

$$k_\perp^2\rho_i^2 \sim (\frac{\omega}{v_A})^2\rho_i^2 < 1 . \quad --(70)$$

It is instructive to compare it with the special case of ion Bernstein wave heating, where

$$k_\perp^2\rho_i^2 \sim \frac{1}{<\rho_i^2>}\rho_i^2 \geq 1, \quad --(71)$$

and asymptotic expansion is used more appropriately:

$$J_n(\frac{1}{2}k_\perp^2\rho_i^2) \sim (\frac{1}{2}k_\perp^2\rho_i^2)^{-1/2} \quad --(72)$$

An interesting aspect of ion Bernstein Wave Heating is that wave interaction reduces as particle energy increases[12] and, hence, it does not have runaway features which is inherent to fast wave heating schemes.

b) Landau damping and Transit time damping

For n=0, we obtain

$$\frac{\partial f}{\partial t} = \frac{\partial}{\partial p_\parallel} D_\parallel \frac{\partial}{\partial p_\parallel} f \quad --(73)$$

with

$$D_\parallel = \frac{1}{|v_\parallel|}[(\frac{v_\perp}{v_\parallel}J_1 + J_0 \mathrm{Im}(\frac{E_{k,z}}{E_{k,y}}))^2 + (J_0 \mathrm{Re}(\frac{E_{k,z}}{E_{k,y}}))^2]\ |E_y|^2 . \quad ---(74)$$

Equation(15) gives not only dispersion relation Eq.(16) but also gives the interrelationship between electric field components:

$$\frac{E_{k,z}}{E_{k,y}} = \frac{1}{\varepsilon_{zz}}\left(\frac{N_x N_z \varepsilon_{x,y}}{\varepsilon_{xx} - N_z^2} + \frac{\varepsilon_{zx}\varepsilon_{xy}}{\varepsilon_{xx} - N_z^2} - \varepsilon_{zy}\right) \quad --(75)$$

By substituting Eq.(75) into Eq.(74), we get

$$D_{\parallel} = \frac{1}{4}\left(\frac{k_{\perp}^2}{\omega_{c,e}^2}\right)\left(v_{\perp}^2 - v_{th,e}^2 - 2\frac{\omega^2 c^2}{\omega_{p,e}^2}\right)^2 |E_y|^2. \quad --(76)$$

The term proportional to $v_{\perp}^2$ comes from transit time damping and the last term comes from Landau damping. It is instructive to calculate power absorbed by electrons,

$$P = \int_{-\infty}^{+\infty} dv_{\parallel} \int_{0}^{\infty} 2\pi v_{\perp} dv_{\perp} \left[\frac{1}{2} m v_{\parallel}^2 \frac{\partial f}{\partial v_{\parallel}}\right], \quad --(77)$$

which reduces to following simple form after straight forward calculation.

$$p = \frac{\sqrt{\pi}}{V}\frac{\varepsilon_0 c^2}{v_{th}}\frac{\omega^2}{\omega_c^2}\int \frac{d^3k}{(2\pi)^3}\frac{k_{\perp}^2}{|k_{\parallel}|}|E_y|^2\left(\alpha + \frac{1}{\alpha}\right)\exp\left(-\frac{m}{2T}\left(\frac{\omega}{k_{\parallel}}\right)^2\right) \quad --(78)$$

Here, we put

$$\alpha = \frac{\omega_p^2}{\omega^2}\frac{T}{mc^2}. \quad --(79)$$

Then, $\alpha > 1$ and $\alpha < 1$ corresponding to transit time damping and Landau damping, respectively. It is clear that transit time damping becomes more important as the plasma beta increases[13]. Most of the present experiments are at the bottom of the α-dependence as drawn in Fig.10.

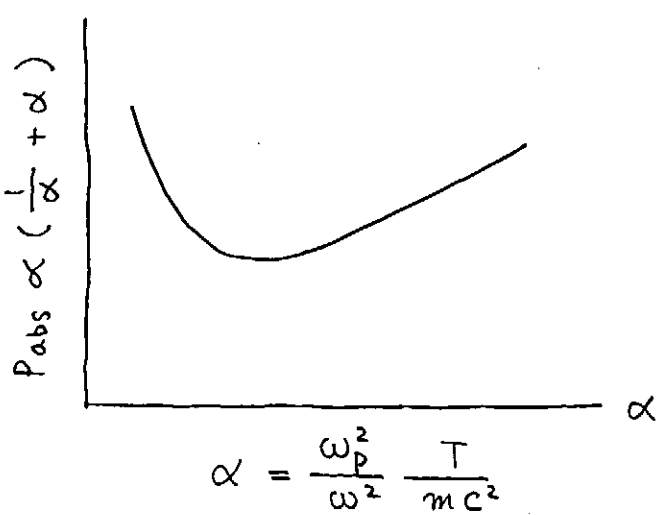

Fig.10: α-dependence of the wave absorption interaction

Part-II Current Drive

II.1 Current drive with low phase velocity wave

In neo-classical theories, ohmically driven current is expressed in the form of

$$\langle J \cdot B \rangle = \sigma \langle E \cdot B \rangle \quad --(101)$$

which means that the inductive electric field gives electron momentum parallel to the magnetic field to drive the current against the momentum loss due to collisions. Non-inductively driven current and its efficiency are also obtained in an analogy of ohmic current drive, which is valid particularly for waves with slow velocity satisfying

$$v_{\parallel} \ll v_{th}. \quad --(102)$$

The momentum loss of current carrying electrons by collision with ions is given by

$$\delta p_{\parallel} = -(nmv_d)\nu\delta t = (\frac{J}{e})m\nu\delta t \quad --(103)$$

and the momentum input to the electrons from the wave is given by

$$\delta p_{\parallel} = (\frac{\delta p_{\parallel}}{\delta E})(\frac{dE}{dt})\delta t = \frac{k_{\parallel}}{\omega} P\delta t \quad --(104)$$

as illustrated in Fig.8. Current drive efficiency J/P is obtained by equating (103) and (104):

$$\frac{J}{P} = \frac{e}{m\nu}\frac{k_{\parallel}}{\omega} = \frac{e}{m\nu v_{\phi\parallel}} . \quad --(105)$$

Saving rigorous discussions, we simply put

$$\nu = Z_i \nu_0 \quad --(106)$$

to obtain

$$\frac{J}{P} = \frac{env_{th}}{nmv_{th}^2 \nu_0}\frac{1}{Z_i}(v_{\phi\parallel}/v_{th})^{-1} . \quad --(107)$$

There are normalizations which are conventionally used by theorists:

$$\tilde{p} = P/nmv_{th}^2 v_0 \ , \ \tilde{j} = J/envth \ , \text{ and } \ w = v_{\phi\parallel}/v_{th} \qquad --(108)$$

with which normalized current drive efficiency is given by

$$\frac{\tilde{j}}{\tilde{p}} = \frac{1}{Z_i} w^{-1} \ . \qquad --(109)$$

It is pointed out that the slower the phase velocity is the higher is the current drive efficiency. This feature comes from the fact that the ratio of the momentum input to the energy on wave particle interaction is given by $k_{\parallel}/\omega$.

Practically, $\tilde{j}/\tilde{p}$ may not be very meaningful. However, if needed, it can be converted to I/P by the formula

$$I/P = \frac{0.77T_e[\text{keV}]}{(n_e/10^{20}[m^{-3}])\log\Lambda} \frac{\tilde{j}}{\tilde{p}} \ . \qquad --(110)$$

II.2 Current drive efficiency for high velocity wave.

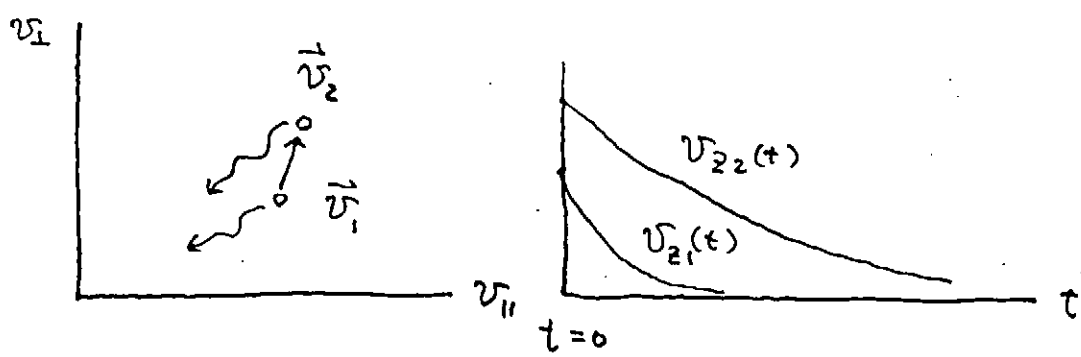

Fig.11 Momentum and energy conservation on wave particle interaction

Current drive efficiency for high velocity wave was obtained by Fisch et al[14]. Consider a case where particle is kicked in velocity space in wave particle interaction as shown in Fig.8, where an electron gains momentum

$$\delta p_{\parallel} = p_{\parallel,2} - p_{\parallel,1} \qquad --(111)$$

and momentum

$$\delta E=E_2-E_1 \ . \quad --(112)$$

Since electrons carries current induced by the velocity increment for the period of $1/\nu$, the induced current will be given by

$$J(t)=-e\int_{-\infty}^{t}\frac{dn(t')}{dt}[v_{z2}\exp(-\nu_2(t-t'))-v_{z1}\exp(-\nu_1(t-t'))]dt' \quad --(113)$$

which is integrated to yield

$$J=-e\frac{dn}{dt}(v_{z,2}/\nu_2-v_{z,1}/\nu_1) \ . \quad --(114)$$

The power flow from the wave to electrons is given by

$$P=\frac{dn}{dt}(E_2-E_1) \ . \quad --(115)$$

From Eqs.(114) and (115), we get the current drive efficiency

$$\frac{J}{P}=-e(\frac{v_{z2}/\nu_2-v_{z1}/\nu_1}{E_2-E_1}) \quad --(116)$$

which reduces to

$$\frac{J}{P}=-e(\frac{\vec{s}\cdot\nabla(v_z/\nu)}{\vec{s}\cdot\nabla E}) \quad --(117)$$

for infinitesimally small kick of the particles.

II.3 Elaboration of the calculation of current drive efficiency.

We assumed ν~const to obtain Eq.(117) which was a little too crude approximation. We see in the following calculation that the temporal change of the collision frequency gives non ignorable correction to the current drive efficiency[15]. We start with two coupled equations

$$\frac{dw}{dt}=-\frac{1}{\tau_s}w \quad --(118)$$

with

$$\tau_s = \frac{\tau_0}{2+Z_i} u^3 \quad . \quad --(119)$$

The energy relaxation of electron may be written as

$$\frac{d}{dt}\left(\frac{1}{2}u^2\right) = -\frac{1}{\tau_E}\left(\frac{1}{2}u^2\right) \quad --(120)$$

with

$$\tau_E^e = \frac{1}{2}\tau_0 u^3 \quad . \quad --(121)$$

These coupled equations are integrated to give

$$v_z(t) = v_{z,0}\left(1 - \frac{3\nu_0}{u_0^3}(t-t_0)\right)^{\frac{2+Z_i}{3}} \quad . \quad --(122)$$

The driven current at t=t is given by

$$J = e\int_{-\infty}^{t} dt' \frac{dn(t')}{dt'}\left(v_{z,2}(t,t') - v_{z,1}(t,t')\right) \quad --(123)$$

which is integrated to give

$$J = e\frac{dn}{dt} v_{th,e} \frac{1}{\nu_o} \frac{1}{5+Z_i} (\delta v\vec{s}) \cdot \nabla (wu^3) \quad . \quad --(124)$$

On the other hand, power absorbed by electron is given

$$P = \frac{dn}{dt} m_e v_{th,e}^2 (\delta v\vec{s}) \cdot \nabla \left(\frac{1}{2}u^2\right) \quad . \quad --(125)$$

Current drive efficiency is thus obtained from Eqs.(124) and (125) as:

$$\frac{J}{P} = \frac{ev_{th,e}}{mv_{th,e}^2 \nu_0} \frac{\tilde{j}}{\tilde{p}} \quad --(126)$$

with

$$\frac{\tilde{j}}{\tilde{p}} = \frac{2}{5+Z_i} \frac{\vec{s}\cdot\nabla(wu^3)}{\vec{s}\cdot\nabla(u^2)} \quad . \quad --(127)$$

For LHCD, where Landau damping is the wave absorption mechanism, put $\vec{s} = \hat{z}$ and get

$$\frac{\vec{j}}{\tilde{p}} = \frac{2}{5+Z_i}\frac{u^3+3uw^2}{2w} \approx \frac{4w^2}{5+Z_i} \quad --(128)$$

Here, we assumed w ~ u, which is valid for LHCD where the velocity of launched wave is much faster than thermal electron speed.
Similarly, for ECH, put $\hat{s} = \perp$ and

$$\frac{\vec{j}}{\tilde{p}} = \frac{2}{5+Z_i}\frac{uu_\perp w}{2u_\perp} \approx \frac{3w^2}{5+Z_i} \quad --(129)$$

is obtained[16]. Here, we notice that the current drive efficiency of ECCD is comparable to that of LHCD, i.e.,

$$(\frac{\vec{j}}{\tilde{p}})_{ECCD} = \frac{3}{4}(\frac{\vec{j}}{\tilde{p}})_{LHCD} \quad --(130)$$

though electron cyclotron damping gives small momentum input to the electron. This is one of the interesting points in kinetic or neoclassical theory.

II.4 Bridge formula

In sections II.1, II.2, and II.3, current drive efficiency was obtained for two limiting case of high phase velocity and low phase velocity . A formula to bridge these results was obtained by Ehst et al. [17,18]:

$$(\frac{\vec{j}}{\tilde{p}})^* = CMR\eta_0 \quad ---(131)$$

Here,

$$\eta_0 = [\frac{K}{w} + D + \frac{4w^2}{5+Z_i}] \quad ---(132)$$

is regarded as the current drive efficiency valid for all regimes with parameters

$$K = (3.0/Z_i) \text{ for LD}, \quad = 11.91/(0.678+Z_i)) \text{ for AW} \quad ---(133)$$

and

$$D = 3.83/Z^{0.707} \text{ for LD, } = 4.131/Z^{0.707} \text{ for AW.} \quad --(134)$$

The factor

$$C = 1 - \exp(-(cy_t)^m) \quad --(135)$$

reflects the fact that trapped particles cannot carry current. Other parameters are:

$$m = 1.38 \text{ for LD, } = 2.48 \text{ for AW} \quad --(136)$$

$$c = 0.389 \text{ for LD, } = 0.0987 \text{ for AW.} \quad --(137)$$

The value of B included in

$$y_t = w^2(B/B_M)/(1 - B/B_{max}) \quad --(138)$$

is the magnetic field strength at the place where the wave particle interaction takes place. The other parameters are not of interest to us and are noted below without explanation:

$$M = [1 + a(\lambda_t/w)^k]$$

$$\lambda_t^2 = (1 - B/B_{max}),\ k = 3.0$$

$$a = 0.0 \text{ for LD / } 12.3 \text{ for AW}$$

$$R = [1 - \frac{\varepsilon^n \sqrt{X_r^2 + w^2}}{\varepsilon^n X_r + w}],\ X_r = 3.5,\ n = 0.77$$

It is noted that thermal velocity is defined as $v_{th} = T_e/m$ in this section and, therefore, J/P is expressed by

$$\frac{J}{P} = \frac{0.38\, T_e[\text{keV}]}{(n_e/10^{20}[\text{m}^{-3}])\log\Lambda}(\frac{\hat{j}}{\tilde{p}})^*. \quad --(139)$$

Fig.12 show the current drive efficiency calculated with the bridge formula. It is often used in simulation of current drive for it saves computing time.

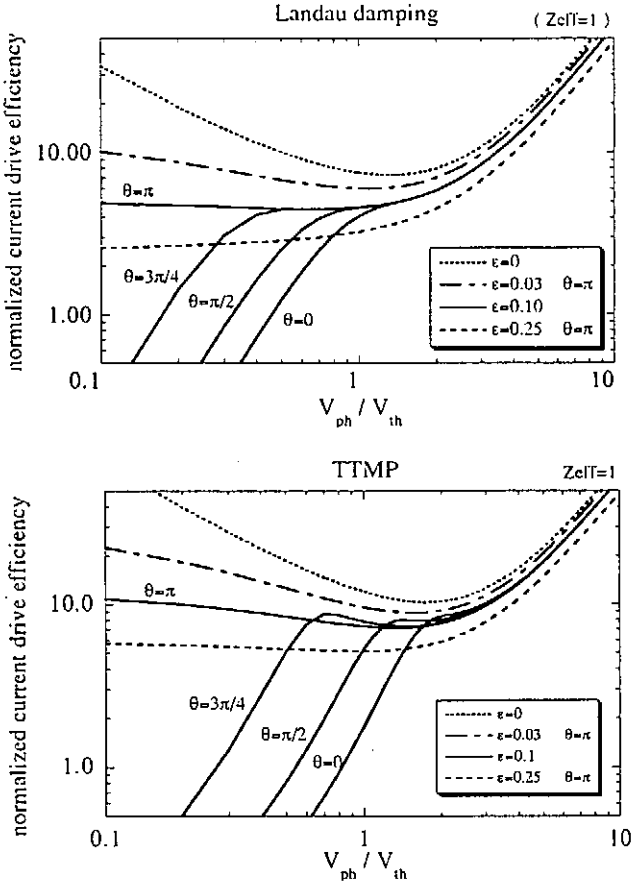

Fig.12 : Current Drive Efficiency Calculated with the Bridge Formula

II.5 current drive figure of merit γ

We have been discussing the current drive efficiency in terms of J/P and $\tilde{j}/\tilde{p}$.
In current drive of tokamaks, we may be the most interested in total current normalized to total input power:

$$\frac{I}{P_{tot}} = \frac{\pi a^2}{(2\pi R)\pi a^2}\frac{J}{P} \quad . \quad --(150)$$

Hereafter, we may be using P in place of P_{total} without confusion. Since the dependence of 1/R in Eq.(150) is inevitable and J/P has a 1/n dependence intrinsically, there is a reason to use the current drive figure of merit

$$\gamma = R(n_e/10^{20}[m^{-3}])\frac{I}{P} . \quad --(151)$$

And, we note that

$$\eta = R(n_e/10^{19}[m^{-3}])\frac{I}{P} \quad --(152)$$

is used similarly; by definition, $\eta = 10\gamma$ $[m^{-2}A/W]$.

II.6 Neutral Beam Injection Current drive.

For self containdness, we refer to NBI current drive which was proposed by T.Ohkawa [19-20] in his old paper and demonstrated in Levitron or DITE tokamak experiment[21-22]. Recently, it was more clearly demonstrated in large tokamaks reporting higher current drive efficiency. Let us consider high energy ions which are steadily supplied by means of parallel NBI. For such ions with $T_h > 15T_e$, ions are dragged by electrons. The number of ions are given by

$$n_h = \frac{1}{\nu_s}\left(\frac{dn}{dt}\right)_{NBI} \quad --(153)$$

carrying the current

$$J_h = Z_h e n_h v_h = \frac{Z_h e v_h}{\nu_s}\left(\frac{dn}{dt}\right)_{NBI} . \quad --(154)$$

Electrons are accelerated by this drag force in the same direction as the hot ions subject to the momentum balance equation:

$$-n_e m_e v_e \nu_{ei} + n_h v_h m_h \nu_s = 0 . \quad --(155)$$

Electron current is given by

$$J_e = n_e(-e)v_e = -e\frac{n_h v_h m_h \nu_s}{m_e \nu_{e,i}} . \quad --(156)$$

Taking into account the relation,

$$\frac{\nu_{e,i}}{\nu_s} = \frac{n_i Z_i^2 \nu_0 / n_e}{(m_e/m_h)Z_h^2 \nu_0} , \quad --(157)$$

it is easily obtained that

$$J = J_h + J_e = en_h Z_h v_h (1 - \frac{Z_h}{Z_{eff}}) . \quad --(158)$$

It is known that a little more effort [23] leads to an elaborated expression

$$J = en_h Z_h v_{h_h} (1 - \frac{Z_h}{Z_{eff}} G) \quad --(159)$$

with

$$G = 1 - (1.46 + 0.976 / Z_{eff}) \sqrt{\varepsilon} \ . \quad --(160)$$

Equation (106) is invalid with large ε and more exact formula are developed by many authors [24].
By using Eq.(153) and obvious relations,

$$P_{NBI} = E_h \frac{dn_h}{dt}; \ E_h = \frac{1}{2} m_h v_h^2 \quad --(161)$$

, current drive efficiency is given by

$$\frac{J}{P} = \frac{1}{\nu_s} \frac{1}{E_h} v_h Z_h e (1 - \frac{Z_h}{Z_{eff}} G) = \frac{en_e v_{th,e}}{m_e n_e v_{th,e}^2 \nu_0} \frac{v_{th,e}}{v_h} \frac{2}{Z_h} (1 - \frac{Z_h}{Z_{eff}} G) \ . \quad --(162)$$

Normalized current drive efficiency is given by

$$\frac{\tilde{j}}{\tilde{p}} = \frac{v_{th,e}}{v_h} \frac{2}{Z_h} (1 - \frac{Z_h}{Z_{eff}} G) = \sqrt{\frac{T_e}{E_h}} \sqrt{\frac{m_p}{m_e} A_h} \frac{2}{Z_h} (1 - \frac{Z_h}{Z_{eff}} G) \quad --(163)$$

and the current drive figure of merit is given by

$$\gamma = 0.0081 T_e [keV] \sqrt{\frac{T_e}{E_h}} \sqrt{\frac{m_p}{m_e} A_h} \frac{2}{Z_h} (1 - \frac{Z_h}{Z_{eff}} G) \ . \quad --(164)$$

II.7 Experimental results:

Since current drive is critically important in realization of steady state tokamak reactors, it was examined in many tokamak experiments. Particularly, attention was paid to the improvement of current drive efficiency. The experimental results obtained in such experiments are summarized in Fig.13. We notice first of all that the 1/n dependence of the CD efficiency predicted theoretically in the previous section manifests itself.

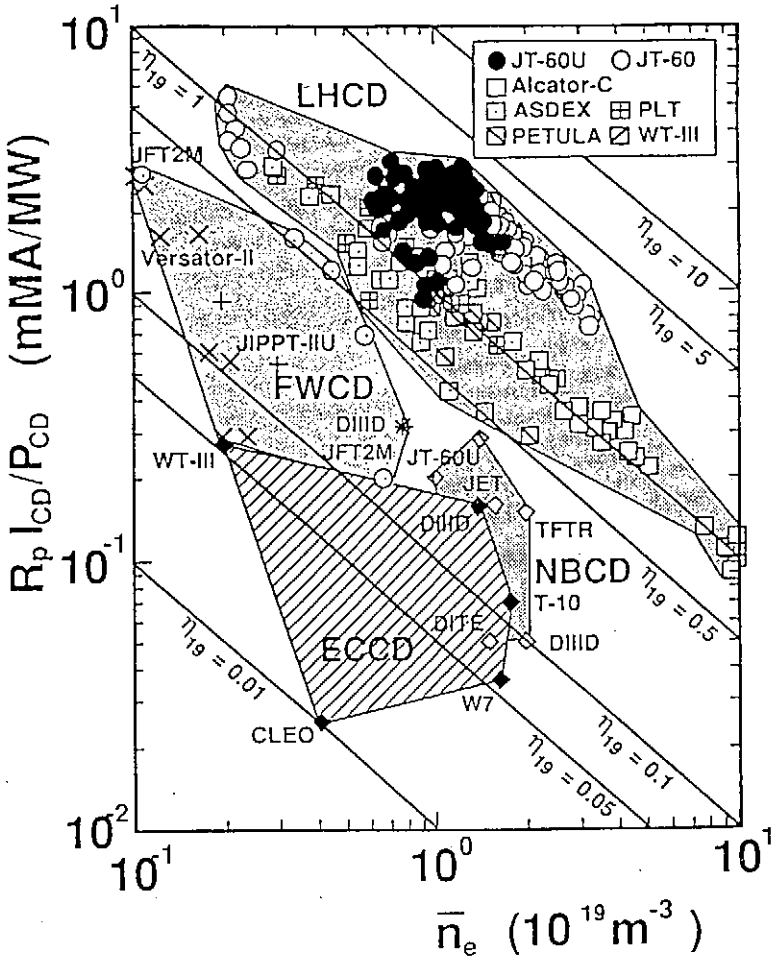

Fig.13 Efficiency of various current drive schemes

1. LHCD

The most established current drive scheme is Lower Hybrid Current Drive[25]. The current drive figure of merit γ increased in the recent experiments in Large tokamaks, JT-60[26-27] and JET[28]; the highest value ever achieved is $\gamma = 0.35$. Experimentally obtained CD efficiency is plotted in Fig.14 versus Te. We find, in Fig.14, another prominent feature that CD efficiency depends on electron temperature, which contradicts with the theoretical predictions of previous section. It is suggested that the readers confirm that Te included in Eqs .(110) is canceled when Eq.(128) is substituted.

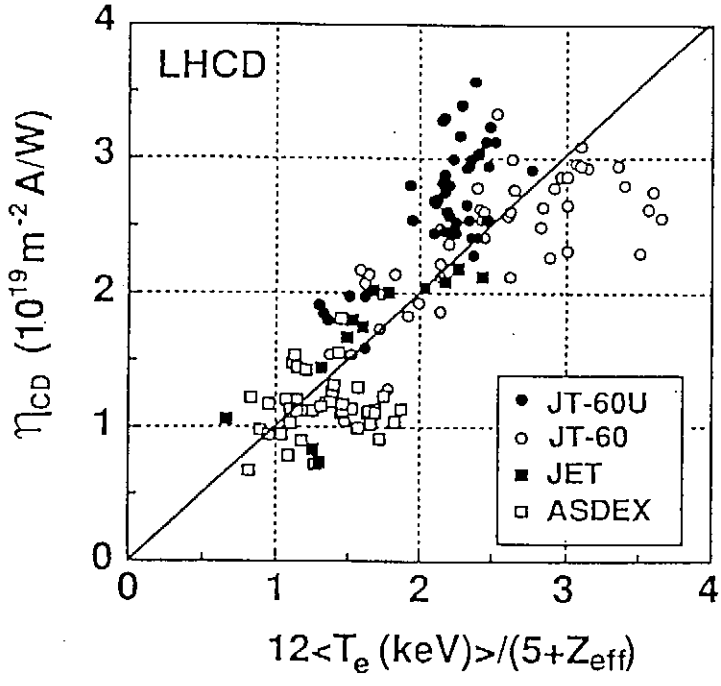

Fig.14 : Temperature Dependence of LH Current Drive

We obtain from Fig.14 an empirical scaling law for the LHCD of a form

$$\gamma = \frac{1.2 < T_e [\mathrm{keV}] >}{5 + Z_{\mathrm{eff}}} \quad . \quad --(180)$$

On the other hand, by using Eq.(128) for LHCD together with Eqs.(110) and (151), three theoretical expressions are obtained:

$$\gamma = 0.033 T_e [\mathrm{keV}] \frac{1}{5 + Z_i} \left(\frac{v_z^2}{v_{\mathrm{th,e}}^2} \right), \quad --(182)$$

$$\gamma = \frac{8.3}{5 + Z_i} \frac{1}{N_{\parallel}^2}, \quad --(183)$$

and

$$\gamma = 0.0081 T_e[\mathrm{keV}] \frac{\tilde{j}}{\tilde{p}} \quad . \quad --(184)$$

Here, we assumed $\log\Lambda = 15$.
Comparing Eqs.(182)-(184) with Eq.(180), we obtain following values

$$(v_{\parallel}/v_{th,e}) \sim 6 \quad --(185),$$

$$n_{\parallel} = 2.6 \quad --(186),$$

and

$$\frac{\tilde{j}}{\tilde{p}} \sim 25 \quad . \quad --(187)$$

Here, a likely electron temperature $< T_e > \sim$1keV has been assumed. Eq.(185) means that the wave is interacting with the small population of electrons with energy level ~ 80keV. Equation (186) needs some explanation because the phasing of the LHCD wave launcher gives a spectrum where $N_{\parallel} < 2$. A probable explanation is that the upshift of the wave number occurs as the wave propagates into the plasma.

2. FWCD

As we will see later, LHCD is known to have density limit. Fast wave current drive has not fully proven its usefulness yet. We have seen in Fig.13 the lower efficiency of FWCD compared with that of LHCD. However, due to its expected better accessibility to the plasma core under a reactor plasma condition, FWCD is regarded as one of the hot themes of investigation. There are some early works in this field and it is becoming clear that considerably high electron temperature is needed to obtain detectable current drive efficiency[29-32]. We can take FWCD efficiency data ,for example, from[32], and deduce an empirical law

$$\gamma = \frac{0.071 < T_e >}{5 + Z_i} \quad . \quad --(190)$$

Direct comparison of Eq(180) with Eq(190) suggest that current drive efficiency of FWCD is worse by more than an order of magnitude compared to that of LHCD. Theoretically, we may employ Eq.(128) as approximate normalized current drive efficiency for both LHCD and FWCD. The , Eqs.(182~184) are valid for FWCD too and gives three values corresponding to Eqs.(185-187):

$$(v_{\parallel}/v_{th,e}) \sim 1.5 \quad --(191)$$

$$n_{\parallel} = 6 \quad --(192)$$

and

$$\frac{\tilde{j}}{\tilde{p}} \sim 1.35 . \quad --(193)$$

Here, we assumed $< T_e > \sim 1.5$keV.

Notable difference of FWCD from LHCD is that the wave interacts with electrons with thermal velocity, as is clear in the comparison of Eq.(185) and Eq.(191). In the discussions above, we have been implicitly adopting a hypothesis that the wave upshifts its $N_{\parallel}$ until enough number of electron exists to absorb the waves. It is known that FW is electromagnetic wave whose interaction with electrons is weaker than that of LHW. In order for the fast wave to have strong enough interaction, FW has to slow down so as to interact with more electrons with a matched speed.

3. ECCD

Demonstration of ECCD has been made in various devices: Cleo, WT-III[33], DIII-D[34], and T-10[35]. Here, we take one example from DIII-D and take current drive efficiency

$$\gamma = \frac{0.03 < T_e >}{5 + Z_i} . \quad --(194)$$

We have already taken in the previous section that the current drive efficiencies for FWCD and LHCD have similar form. ECCD relies on cyclotron damping or higher harmonic damping for the wave damping mechanism.Two important differences of ECCD from others are 1) that the direction of the kick is dominantly perpendicular and 2) that the resonance condition is given by

$$k_{\parallel} v_{\parallel} = \omega - \omega_{c,e} . \quad --(195)$$

The resonance layer is located on the axis of the plasma in the standard experimental condition. The wave interacts with electrons with positive $v_{\parallel}$ with respect to the direction of wave propagation as it propagates in the low field side and it interacts with electrons with negative $v_{\parallel}$ in the low field side. If wave absorption in one pass through the resonance layer is not strong enough, canceling of the current drive occurs to reduces the efficiency. This may have made analyses of ECCD in small devices difficult.

A simple form of ECCD figure of merit envisaged from Eq.(129) will be

$$\gamma = \frac{3}{4} \frac{8.3}{5 + Z_i} \frac{1}{N_{\parallel}^2} \left(1 - \frac{\omega_{c,e}}{\omega}\right)^2 \quad --(196)$$

or equivalently

$$\gamma = \frac{3}{4} 0.033 T_e [\mathrm{keV}] \frac{1}{5 + Z_i} \left(\frac{v_z^2}{v_{th,e}^2} \right) . \quad --(197)$$

Comparison of Eq.(194) with Eqs.(196-197), gives

$$(v_{\parallel} / v_{th,e}) \sim 1.2 \quad --(198)$$

,

$$N_{\parallel} = 12 \left| 1 - \frac{\omega_{c,e}}{\omega} \right| \quad --(199)$$

, and

$$\frac{\tilde{j}}{\tilde{p}} = 0.57 . \quad --(200)$$

Eq.(198) suggests that the EC wave interacts with electrons of thermal speed. And since

$$N_{\parallel} \sim \sin\vartheta \sim 0.5 \quad --(201)$$

, Eq.(199) suggests that wave is absorbed in the very thin layer near the cyclotron resonance.

II. 8 Requirement to the figure of merit γ

Let us imagine a model tokamak reactor as shown in Fig.15 and consider a set of parameters tabulated in table-1, for which the exact values are not be important.

I_p=15MA	$P_{electric}$=1GW	$P_{thermal}$=2GW	Circulating Power=200MW
Major radius R=8m	Minor radius a=2m	Density n=1020 m-3	Electron Temperature T_e=10keV

Table-1 A set of parameters of a typical reactor

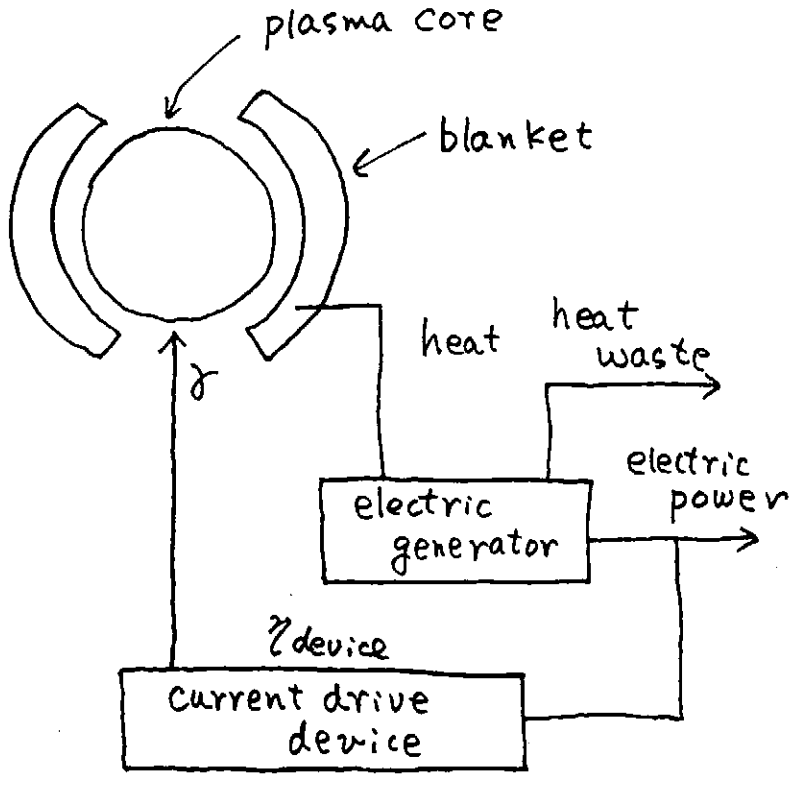

Fig.15 A model of a reactor with current drive

Figure 15 immediately suggests that we can obtain a reactor requirement

$\gamma = 1.2$. --(210)

by use of Eq.(151) with the values listed in Table .1. This is three times larger than the largest value ever achieved in LHCD experiments. For the reason we will discuss later, this requirement may be difficult to achieve and the boot-strap current may have to take over some fraction of the plasma current.

II.6 Perspective of Current Drive Schemes

1. LHCD.

As we have seen in section II.7, γ_{LHCD} is higher than γ_{FWCD} and γ_{EC} by at least by an order of magnitude. And also, we realize that we have to improve the current drive figure of merit by three times over the presently obtained value. Is it possible? The empirical scaling law suggest that the current drive efficiency increases as Te increases: a direct extrapolation of the empirical scaling law suggests that the current drive efficiency will be improved by several times over the presently obtained value. However, this extrapolation may not be adequate.The theoretical expression Eq.(183) has $(1/N_{\parallel})^2$ dependence in place of $< T_e >$ dependence in the experiment.

This discrepancy may be explained in terms of wave spectrum upshift. A very unique feature of Lower Hybrid Current Drive is that LHW has strong interaction with electrons and it may have

allowed the wave to interact with electrons with the wave with $N_{\parallel} \sim 2.6$ giving higher CD efficiency than others. In a reactor condition where a higher electron temperature is expected, there is a possibility that wave is absorbed before it makes upshift improving CD efficiency. However, we have to pay attention to the fact that the LHW is interacting with high energy electrons of ~80keV with reasonably low $N_{\parallel}$~2.6 even in the existing devices. If we want to reduce $N_{\parallel}$ further in order to increase γ, we have to examine the wave accessibility condition. Also, when we work with low $N_{\parallel}$ or high speed electrons, relativistic effects have to be considered. As introduced in appendix, inclusion of the relativistic effect reduces the current drive efficiency considerably for $N_{\parallel}$ smaller than $\sqrt{2}$.

2. FWCD

FWCD is still in the developmental phase. The achieved γ is one order of magnitude lower than that of LHCD. In the D-IIID experiment for example, the wave interacts with electrons of $v_{\parallel}/v_{th,e}$~1.5 as we saw in Eq.(191). Associated interpretation is that the wave $N_{\parallel}$ upshifted to 6 before it is absorbed. To describe in more detail, we should know that the wave spectrum of the fast wave is adjustable by changing the relative phase of antenna array or changing the frequency of the RF frequency applied to the antenna system. It is more or less believed that it is necessary to choose wave phase velocity not much above thermal speed. This is a feature completely different from LHCD. In this experiment, wave spectrum has a peak around $N_{\parallel} = 4 \sim 5$ as it is emitted from the wave launcher. Such interpretation of the FWCD experiments suggests that the wave $N_{\parallel}$ can be decreased as the electron temperature increases in a reactor plasma where more of the electrons match the velocity of the wave. This may increase the current drive efficiency up to the level expected for LHCD. FWCD has a smaller wave accessibility problem than LHCD. Yet, there is a question of what frequency to choose: Since we want to make electrons absorb wave energy, it is very natural to avoid the presence of fundamental frequency of fuel ions, i.e., $\omega = \omega_{c,D}$ or $\omega = \omega_{c,T}$. If we go to higher frequency, the absorption by each harmonic resonance layer becomes weak. However, we may have to keep in mind the presence of alpha particles, product of nuclear fusion reaction. Alpha particles have higher energy than fuel ions and, due to its larger finite Larmour effect than that of fuel ions, interaction with Alpha-particles survive even with a frequency of very high harmonic number[36].

Fig.16 shows the calculation of partition of the wave energy to plasma species. Apparently, in the frequency range of $\omega < \omega_{c,T}$, there is no ion heating mechanism. Therefore, this frequency range is one of the candidates of the fast wave current drive. A little concern is however the presence of the cut off and resonance layers at the high field side, whose existence is already seen in Fig.6 qualitatively . Another problem is that a large antenna area is required when the RF frequency is low. Another possibility is the frequency window between $2\omega_{c,T}$ and $3\omega_{cD}$ where, though some wave energy is absorbed by ions, major part of it is absorbed by electrons.

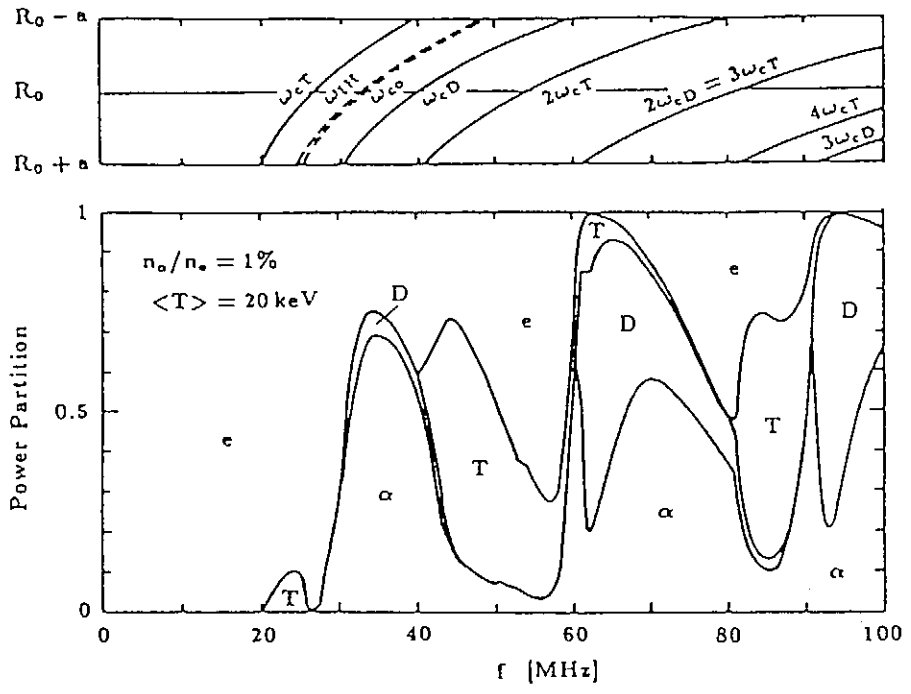

Fig.16 : Partition of wave power to electrons , ions, and α-particles

3. ECCD

Electron Cyclotron Current Drive has similar current drive efficiency as FWCD, one order of magnitude lower than that of LHCD as shown in Fig.13. Similarly to the FWCD case, this relatively low efficiency is attributed to the low energy of electrons taking part in the wave particle interaction. Equation.(198) suggest that $v/v_{th,e} \sim 1.2$.

In ECCD, wave interacts with electrons with parallel velocity

$$v_{\parallel} = (1 - \omega_{c,e}/\omega)c/N_{\parallel} \quad . \quad --(212)$$

In present day tokamaks, there is a low population of high energy electrons and $N_{\parallel}$ is intrinsically small due to the design of the wave injector. Equation (212), therefore, suggests that wave absorption occurs only near the resonance region. However, in a reactor condition with its higher temperature and larger length crossing the minor radius, the wave is expected to be absorbed away from the resonance region increasing the current drive efficiency up to the level of LHCD.

ECCD has no big problem in wave accessibility only if high frequency gyrotron is developed. Further more it has a merit of being capable of define the deposition profile in its advanced use of improving reactor performances. Therefore, development of high frequency-, high power-, and, steady state- gyrotron is important as well as the establishment of current drive physics itself.

II.10 Boot strap current

In the previous section we studied that the current drive efficiency may not be improved very much over the current drive efficiency ever achieved. On the other hand presence of boot strap current is becoming more and more evident[38]. Bootstrap current has an expression[37]:

$$<j\cdot B> = -RB_t n_e \sum_s \frac{T_s}{Z_s}\left[L_{31}^s \frac{\partial \ln P_s}{\partial \psi} + L_{32}^s \frac{\partial \ln T_s}{\partial \psi}\right]. \quad --- \quad (220)$$

Heuristically, they assume $L_{32}^s = 0$ and put

$$L_{31} = \sqrt{r/R} \quad --(221)$$

for a large aspect tokamak of circular cross section to obtain

$$j_{\parallel} = -\sqrt{r/R}\,\frac{1}{B_p}\frac{dP}{dr} \quad --(222)$$

The total current I is obtained by

$$I = \int <j\cdot B> \frac{\vec{B}}{<B^2>}\cdot d\vec{s} \approx \int -\sqrt{r/R}\,\frac{1}{B_p}\frac{dP}{dr}\,2\pi r dr \quad --(223)$$

In the original papers on boot-strap current, it was stated that the total fraction of the boot strap current is given by

$$I_{bs}/I \sim \sqrt{\varepsilon}\,\beta_p \quad --(224)$$

For tokamaks, there have been a class of papers to search for the pressure profile to maximize beta-value under the constraint of ballooning stability.
In the recent works in tokamaks, there is more freedom in current profile and pressure profile than they admitted at that time and such freedom could be used for optimization of the boot strap current.
Let us define the boot strap current fraction by

$$f_B = I_{bootstrap}/I_{total} \quad . \quad --(225)$$

It is accepted these days that $f_B \sim 0.7$ is obtained without adopting too innovative profile control.
The power required for current drive for a reactor modeled in Fig.15 is given by

$$P = \frac{1}{\eta_{device}} \ln R \frac{(1 - f_B)}{\gamma} \quad . \quad --(226)$$

With the model reactor parameters listed in Table.1 and assumed $f_B \sim 0.7$, required current drive figure of merit γ goes down to 0.4, which is not very much different from the value obtained presently for LHCD.

III. Discussions

As discussed in the text, achievable current drive efficiency is not high enough to sustain a steady state tokamak alone. Recently, presence of boot strap current is more and more evident and it is believed that 70 % of total current will be undertaken by the boot strap current. Boot strap current, however, is driven by pressure gradient necessarily determining the current profile. The boot strap current is known to be hollow, and remaining 30 percent of current has to be driven in the central region and, depending on the pressure profile, some current has to be driven in the peripheral region. Fast wave current drive is known to have excellent accessibility to the plasma core. However, due to the general feature of the fast wave that it has weak interaction with particles, demonstration of it's validity was difficult. It is believed to work under a reactor conditions where electron temperature is higher and the size of the devices larger. Readers are requested to recall the "golden rule" mentioned at the beginning of this course. ECCD has also good accessibility to the plasma core though the development of gyrotron at high frequency is difficult. Thanks to the devotion of many scientists, the power and steady state capability of gyrotron is increasing. The efficiency of the gyrotron is presently 40 percent at most. More works has to be done to improve the efficiency. In order for NBCD to be used as a tool to drive current in the plasma core, it is important to increase the energy of the injection beam. Development of high current negative ion beam is mandatory and considerable progress was made. People are thinking of the energy level of 1MeV for ITER NBI. More technology development has to be done to enable acceleration up to such high energy. Lower hybrid current drive cannot be a good candidate of core current driver unless a reactor is designed with much higher magnetic field. It is a recent trend of study to create negative shear of the magnetic field which means very hollow current profile. LHCD is expected to be a good tool to realize such conditions. In general, we have been tailoring the current profile in order to improve energy confinement and in order to increase boot strap fraction. These too optimizations do not seem to be very contradictory. However , more experimental research should be done. Similarly, second stability allows more boot strap fraction and it is again important to examine the compatibility of the boot-strap driven current profile and the equilibrium. One more key factor in the reactor is ash removal though it was not treated here. An interesting proposal made by Fisch is the use of entropy of such particles in order to exhaust themselves. Alfven or IB wave is amplified in return which could be used again in maintaining current. Such passive way of current sustainment is very favorable and further development is recommended.

I.V Appendix

Relativistic effects

High current drive efficiency is obtained when the wave couples with high-energy electrons because the momentum loss of such electrons is small. This effect overcompensates small specific momentum input and yields following favorable dependence on $v_{\parallel}$ in classical limit:

$$\frac{\delta J}{\delta P} \propto v_{\parallel}^{-2} . \quad --(230)$$

Such discussion reviewed in section II.2 and II.3 is easily extended to a relativistic case. The expression of the current drive efficiency in relativistic limit was given by Fish et al.[39-40].

$$J/P \simeq \frac{\vec{s} \cdot \frac{\partial g}{\partial p}}{\vec{s} \cdot \frac{\partial}{\partial p}(mc^2\gamma)} \quad --(231)$$

where

$$g(p) = -\frac{ec}{v_c}\frac{p_{\parallel}}{p} G(p) \quad --(232)$$

with

$$G(p) = \left(\frac{\gamma+1}{\gamma-1}\right)^{\frac{1+Z}{2}} \int_0^{\gamma} \left(\frac{\gamma'+1}{\gamma'-1}\right)^{\frac{1+Z}{2}} \frac{\gamma'^2-1}{\gamma'^2} d\gamma' . \quad --(233)$$

Equation (231) reduces to

$$\frac{J}{P}/\left(\frac{-e}{mcv_c}\right) = \gamma\frac{m^2c^2}{p^2} \begin{cases} p\frac{dG}{dp} & (\vec{s} \propto \vec{p}_{\parallel});\ \text{Landau damping} \\ p\frac{dG}{dp} - G & (\vec{s} \propto \vec{p}_{\perp}),\ \text{EC damping} \end{cases} \quad --(234)$$

for Landau damping and electron cycrotron damping cases, respectively.
The current drive efficiency is calculated as functions of $\zeta = p_{\parallel}/mc \simeq p/mc$ for the two cases as shown in Fig.17. It is noted that the current drive efficiency saturates for Landau damping case while it begins to decrease for EC damping case. The saturation of the current drive efficiency comes from the decreasing velocity of electron for given energy . Therefore, $\zeta \sim 1$ may set a limit above which there is no improvement of CD efficiency in relativistic treatment.

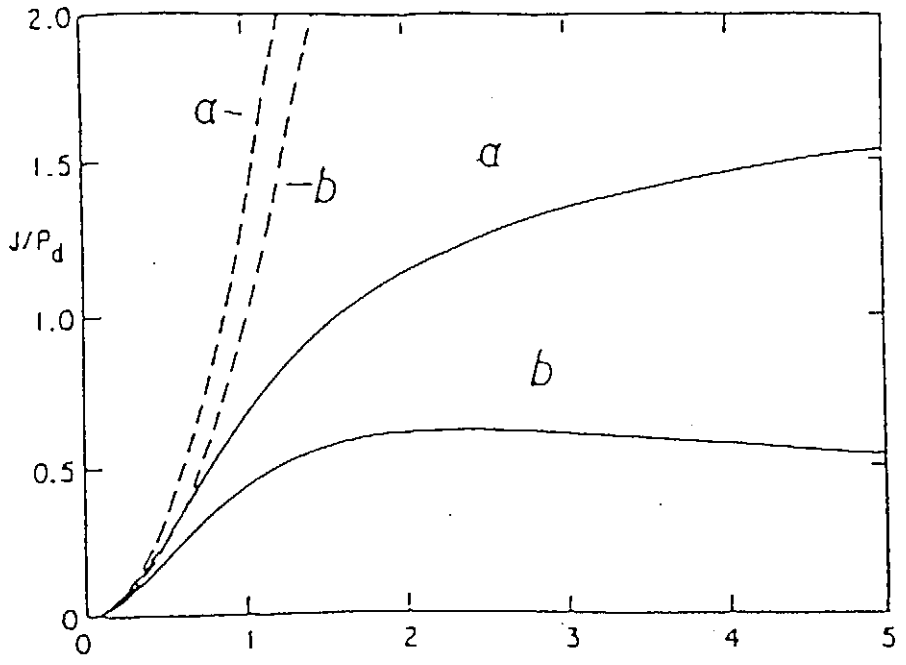

Fig.17 Current drive efficiency of LH and EC current drive cases

Another interesting feature are relativistic modification of the interaction zone and the direction of the kick in the momentum space.
The resonance condition is given by Eq.(61) with relativistic interpretation :

$$\omega - n\omega_{c,0}/\gamma = k_{\parallel} p_{\parallel}/\gamma m_0 \quad --(235)$$

which is reformed to

$$\tilde{p}_{\perp}^2 + (1-N_{\parallel}^2)[\tilde{p}_{\parallel} - \frac{N_{\parallel}^2}{(1-N_{\parallel}^2)}(n\omega_{c,0}/\omega)]^2 + (1 - \frac{1}{1-N_{\parallel}^2}(\frac{n\omega_{c,0}}{\omega})^2) = 0 \quad --(236)$$

manifesting that the resonance is an ellipse in the momentum space. Here, $\tilde{p}_{\perp} = p_{\perp}/m_0 c$ and

$\tilde{p}_{\parallel} = p_{\parallel}/m_0 c$.

The direction of the kick is given by

$$\vec{s} = n\omega_c \hat{e}_{\perp} + k_{\parallel} v_{\perp} \hat{e}_{\parallel} = (\omega - k_{\parallel} v_{\parallel})\hat{e}_{\perp} + k_{\parallel} v_{\perp} \hat{e}_{\parallel} \quad --(237)$$

and interpreted relativistically leading to a differential equation

$$\frac{\delta p_{\parallel}}{\delta p_{\perp}} = \frac{k_{\parallel} v_{\perp}}{(\omega - k_{\parallel} v_{\parallel})} = \frac{\tilde{p}_{\perp}}{((\omega/ck_{\parallel})\gamma - \tilde{p}_{\parallel})} = \frac{N_{\parallel}\tilde{p}_{\perp}}{(\gamma - \tilde{p}_{\parallel} N_{\parallel})} \quad --(238)$$

Equation (238) can be integrated easily to give a family of stream lines in the momentum space. For instance, Fig.17 indicates that electrons gains considerable kick in parallel direction even in ECH, which improves current drive efficiency close to that of Lower Hybrid Current Drive. And more importantly, the stream lines of the electrons in momentum space overlay the resonance region[41,42]. This is expected to be useful in having wave interact strongly with high energy electrons to improve the efficiency.

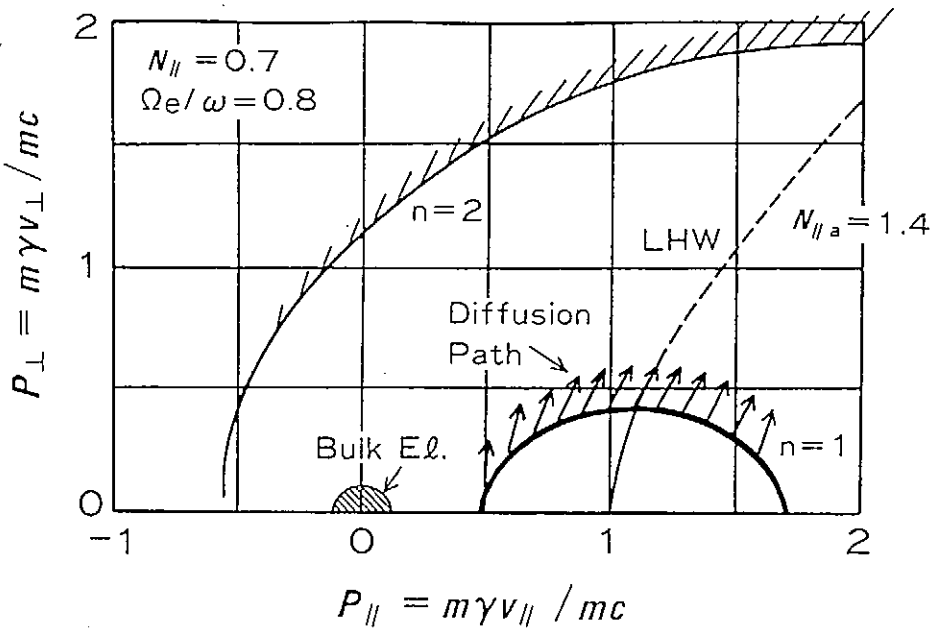

Fig.18 : Wave particle interaction in relativistic regime.

References

[1] Stix, T. H., The Theory of Plasma Waves , McGraw-Hill Book Co. Inc. , New York (1962)

[2] Ichimaru, S., Basic Principles of Plasma Physics -a statistical approach-, W. A. Benjamin Inc., Massachusetts(1973)

[3] Perkins,F.W., Nuclear Fusion, 17(1977)1197

[4] McVey,B.D., Nuclear Fusion, 19(1979)461

[5] Budden,K.G.Radio Waves in the Ionosphere, Cambridge University Press, Cambridge (1961)

[6] Fukuyama, A. et al., Nuclear Fusion, 23(1983)1005
Brambilla, M., Krucken,T., Plasma Phys. Contr. Fus. 30(1988)1083

[7] Jaeger, E.F., et al., Nuclear Fusion, 30(1990)505

[8] Ono, M., Watari, T., et al., Physical Review Letters, 54(1985)2239

[9] Kennel, C.F., Engelmann, F., Physics of Fluids, 9(1966)2377

[10] Montgomery,D., Tidman,D.,Plasma kinetic Theory, McGraw-Hill Book Co., New York(1964)

[11] Stix, T., Nucl. Fusion, 15(1975)737

[12] T. Watari, R. Kumazawa, T. Seki, et al., (proc. 14th international Conference on Plasma Physics and Controlled Nuclear Fusion Research, 1992, Wurtzburg) Vol. 1, p-675
[13] Moreau, D., O'Brien, M.R., Cox, M., (proc. 14th European Conference on Controlled Fusion and Plasma Physics, Madrid, 1987), European Physical Society, 1987, p-1007
[14] Fisch, N.J., Phys.Rev. Letters, 41(1978)873
[15] Karney,C.F.F., Fisch, N.J., Phys.Fluids, 22(1979)1817
[16] Fisch,N.J., Boozer, A.H., Phys.Rev.Letters, 45(1980)720
[17] Ehst, E.D., Karney, C.F.F., Nuclear Fusion, 31(1991)1933
[18] Giruzzi, Nuclear Fusion, 27(1987)1934
[19] Ohkawa,T., Nuclear Fusion, 10(1970)185
[20] Ohkawa, Kakuyugo Kenkyu, 32(1974)1 and 67
[21] Start, D.F., et al., Phys. Rev. Letters, 40(1978)1497
[22] Clark, W.H.M., et al., Phys. Rev. Letters, 45(1980)1101
[23] Start, D.F.H., Cordey, J.G., and Jones, E.M., Plasma Physics, 22(1980)303
[24] Taguchi, M., Plasma Physics.Contr.Fusion,
[25] Yamamoto,T., et al., Phys.Rev. Letters, (1980)716
[26] Usigusa, K., Journal of Plasma and Fusion Research, vol.70, 850p (1994)
[27] Imai, T., et al., (in proc. 13th IAEA Conference on Plasma Physics and Controlled Thermo-Nuclear Fusion Research, Washington, 1990) , IAEA, 1991, Vol.1, p-657
[28] JET team,presented by C. Gormezano (in proc. 14th IAEA Conference on Plasma Physics and Controlled Thermo-Nuclear Fusion Research, Wurzburg, 1992) , IAEA, 1993, Vol.1, p-587
[29] Uesugi,Y., et al., Nuclear Fusion,30(1990)279
[30] Seki, T., Nuclear Fusion, 31(1991)1369
[31] Ohkubo,K. et al., physical Rev. Letters, 56(1986)2040
[32] Petty,C.C., Pinsker, R.I., et al., Nuclear Fusion, 35(1995)773
[33] Tanaka, H., et al., (proc. of the 11th IAEA Conf. on Plasma Physics and Controlled Nuclear Fusion Research, 1986, Tokyo), IAEA, 1987,vol.1, p-553
[34] Luce et al., (proc. of the 13th IAEA Conf. on Plasma Physics and Controlled Nuclear Fusion Research, 1990, Tokyo), IAEA, 1991,vol.1, p-641 DIII-D ECCD
[35] K.A.Razumova, Alikaev, V., et al., Plasma Physics 1(1994)1554
[36] K. Hamamatsu, A.Fukuyama et al., "Theory of Fusion Plasmas" (proc., International School on Plasma Physics, Varrena, 1992), Association Euratom, 1993 p-279
[37] Hirshman,S.P., Sigmar, D.J., Nuclear Fusion, 21(1981)1079
[38] Zarnstoff.C.M., et al., Phys. Rev. Letters, 60(1988)1306 TFTR bootstrap
[39] Karney,C.F.F., Fisch,N.J., Physics of Fluids, 28(1985)116
[40] Fisch, N.J., Phys.Rev. Lett., A24(1981)3241
[41] Mekawa, T. et al., Phys.Rev.Letters, vol.170,(1993)2561,Maehara, T., et al., Phys.Letters, A208, (1995)143

Publication List of NIFS-PROC Series

NIFS-PROC-1 "*U.S.-Japan on Comparison of Theoretical and Experimental Transport in Toroidal Systems Oct. 23-27, 1989*", Mar. 1990

NIFS-PROC-2 "*Structures in Confined Plasmas –Proceedings of Workshop of US-Japan Joint Institute for Fusion Theory Program–* "; Mar. 1990

NIFS-PROC-3 "*Proceedings of the First International Toki Conference on Plasma Physics and Controlled Nuclear Fusion –Next Generation Experiments in Helical Systems– Dec. 4-7, 1989*" Mar. 1990

NIFS-PROC-4 "*Plasma Spectroscopy and Atomic Processes –Proceedings of the Workshop at Data & Planning Center in NIFS–*"; Sep. 1990

NIFS-PROC-5 "*Symposium on Development of Intensed Pulsed Particle Beams and Its Applications February 20 1990*"; Oct. 1990

NIFS-PROC-6 "*Proceedings of the Second International TOKI Conference on Plasma Physics and Controlled Nuclear Fusion , Nonlinear Phenomena in Fusion Plasmas -Theory and Computer Simulation-*"; Apr. 1991

NIFS-PROC-7 "*Proceedings of Workshop on Emissions from Heavy Current Carrying High Density Plasma and Diagnostics*"; May 1991

NIFS-PROC-8 "*Symposium on Development and Applications of Intense Pulsed Particle Beams, December 6 - 7, 1990*"; June 1991

NIFS-PROC-9 "*X-ray Radiation from Hot Dense Plasmas and Atomic Processes*"; Oct. 1991

NIFS-PROC-10 "*U.S.-Japan Workshop on "RF Heating and Current Drive in Confinement Systems Tokamaks" Nov. 18-21, 1991,* Jan. 1992

NIFS-PROC-11 "*Plasma-Based and Novel Accelerators (Proceedings of Workshop on Plasma-Based and Novel Accelerators) Nagoya, Japan, Dec. 1991*"; May 1992

NIFS-PROC-12 "*Proceedings of Japan-U.S. Workshop P-196 on High Heat Flux Components and Plasma Surface Interactions for Next Devices*"; Mar. 1993

NIFS-PROC-13 『NIFS シンポジウム
「核燃焼プラズマの研究を考える－現状と今後の取り組み方」
1992年7月15日、核融合科学研究所』
1993年7月

NIFS Symposium
"Toward the Research of Fusion Burning Plasmas -Present Status and Future strategy-", 1992 July 15, National Institute for Fusion Science"; July 1993 (in Japanese)

NIFS-PROC-14 "*Physics and Application of High Density Z-pinches*", July 1993

NIFS-PROC-15 岡本正雄、講義「プラズマ物理の基礎」
平成5年度　総合大学院大学
1994年2月
M. Okamoto,
"Lecture Note on the Bases of Plasma Pysics"
Graduate University for Advanced Studies
Feb. 1994 (in Japanese)

NIFS-PROC-16 代表者　河合良信
平成5年度　核融合科学研究所共同研究
研究会報告書
「プラズマ中のカオス現象」
"Interdisciplinary Graduate School of Engineering Sciences"
Report of the meeting on Chaotic Phenomena in Plasma
Apr. 1994 (in Japanese)

NIFS-PROC-17 平成5年度 NIFS シンオジウム報告書
「核融合炉開発研究のアセスメント」
平成5年11月29日-30日　於　核融合科学研究所
"Assessment of Fusion Reactor Development"
Proceedings of NIFS Symposium held on November 29-30, 1993 at National Insitute for Fusion Science" Apr. 1994
(in Japanese)

NIFS-PROC-18 *"Physics of High Energy Density Plasmas Produced by Pulsed Power"* June 1994

NIFS-PROC-19 K. Morita, N. Noda (Ed.),
"*Proceedings of 2nd International Workshop on Tritium Effects in Plasma Facing Components at Nagoya University, Symposion Hall, May 19-20, 1994*", Aug. 1994

NIFS-PROC-20 研究代表者　阿部　勝憲　（東北大学・工学部）
所内世話人　野田信明
平成6年度　核融合科学研究所共同研究［研究会］
「金属系高熱流束材料の開発と評価」成果報告書
K. Abe and N. Noda (Eds.),
"Research and Development of Metallic Materials for Plasma Facing and High Heat Flux Components" Nov. 1994
(in Japanese)

NIFS-PROC-21 世話人：森田　健治（名大工学部）、金子　敏明（岡山理科大学理学部）
「境界プラズマと炉壁との相互作用に関する基礎過程の研究」

研究会報告
K. Morita (Nagoya Univ.), T. Kaneko (Okayama Univ. Science)(Eds.)
"*NIFS Joint Meeting "Plasma-Divertor Interactions" and "Fundamentals of Boundary Plasma-Wall Interactions" January 6-7, 1995 National Institute for Fusion Science*"
Mar. 1995 (in Japanese)

NIFS-PROC-22
代表者　河合　良信
プラズマ中のカオス現象
Y. Kawai,
"*Report of the Meeting on Chaotic Phenomena in Plasma,* 1994"
Apr. 1995 (in Japanese)

NIFS-PROC-23
K. Yatsui (Ed.),
"*New Applications of Pulsed, High-Energy Density Plasmas*";
June 1995

NIFS-PROC-24
T. Kuroda and M. Sasao (Eds.),
"*Proceedings of the Symposium on Negative Ion Sources and Their Applications, NIFS, Dec. 26-27, 1994*", Aug. 1995

NIFS-PROC-25
岡本　正雄
新古典輸送概論（講義録）
M. Okamoto,
"*An Introduction to the Neoclassical Transport Theory" (Lecture note)*, Nov. 1995 (in Japanese)

NIFS-PROC-26
Shozo Ishii (Ed.),
"*Physics, Diagnostics, and Application of Pulsed High Energy Density Plasma as an Extreme State*"; May 1996

NIFS-PROC-27
代表者　河合　良信
プラズマ中のカオスとその周辺非線形現象
Y. Kawai ,
"*Report of the Meeting on Chaotic Phenomena in Plasmas and Beyond, 1995*", Sep. 1996 (in Japanese)

NIFS-PROC-28
T. Mito (Ed.),
"*Proceedings of the Symposium on Cryogenic Systems for Large Scale Superconducting Applications*", Sep. 1996

NIFS-PROC-29
岡本　正雄
講義「核融合プラズマ物理の基礎 - I」
平成 8 年度　総合研究大学院大学　数物科学研究科　核融合科学専攻
1996年 10月
M. Okamoto
"*Lecture Note on the Fundamentals of Fusion Plasma Physics - I" Graduate University for Advanced Studies;* Oct. 1996 (in Japanese)

NIFS-PROC-30

研究代表者　栗下　裕明（東北大学金属材料研究所）
所内世話人　加藤　雄大
平成８年度核融合科学研究所共同研究
「被損傷材料の微小体積強度評価法の高度化」研究会
1996年 10月　9日　於：核融合科学研究所

H. Kurishita and Y. Katoh (Eds.)
NIFS Workshop on Application of Micro-Indentation Technique to Evaluation of Mechanical Properties of Fusion Materials, Oct. 9, 1996, NIFS
Nov. 1996 (in Japanese)

NIFS-PROC-31

岡本　正雄
講義「核融合プラズマ物理の基礎 - II」
平成８年度　総合研究大学院大学　数物科学研究科　核融合科学専攻
1997年 4月
M. Okamoto
"*Lecture Note on the Fundamentals of Fusion Plasma Physics - II*"
Graduate University for Advanced Studies; Apr. 1997 (in Japanese)

NIFS-PROC-32

代表者　河合　良信
平成8年度　核融合科学研究所共同研究
研究会報告「プラズマ中のカオスとその周辺非線形現象」

Y. Kawai (Ed)
Report of the Meeting on Chaotic Phenomena in Plasmas and Beyond, 1996; Apr. 1997 (mainly in Japanese)

NIFS-PROC-33

H. Sanuki,
Studies on Wave Analysis and Electric Field in Plasmas; July 1997

NIFS-PROC-34

プラズマ対向機器・PSI・熱・粒子制御合同研究会報告
平成９年６月27日（金）9:00～16:20
核融合科学研究所・管理棟４F 第１会議室
1997年　10月
T. Yamashina (Hokkaido University)
Plasma Facing Components, PSI and Heat/Particle Control
June 27, 1997, National Institute for Fusion Science
T. Yamashina (Hokkaido University)
Oct. 1997 (in Japanese)

NIFS-PROC-35

T. Watari,
Plasma Heating and Current Drive; Oct. 1997